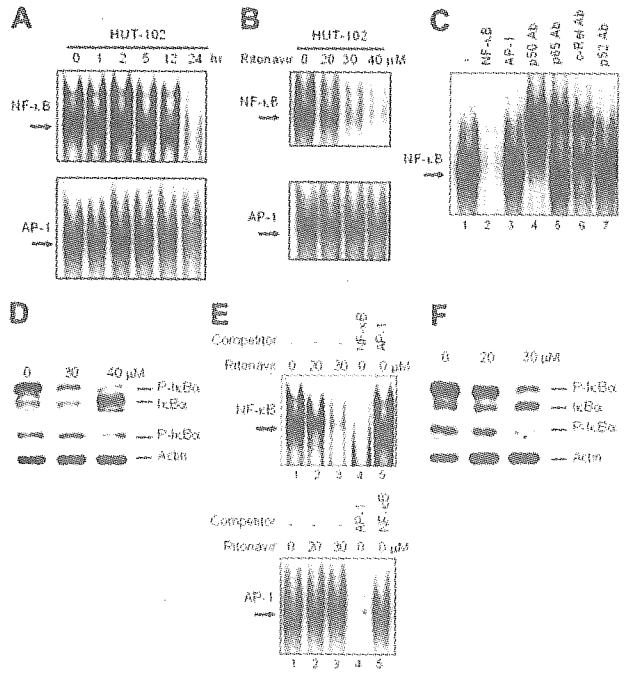

Figure 2. Ritonavir inhibits constitutive NF-κB activation. (A) HUT-102 cells treated with ritonavir (40 μM) for the indicated time were evaluated for NF-κB and AP-1 activation. (B) HUT-102 cells treated with the indicated concentration of ritonavir for 24 hours were evaluated for NF-κB and AP-1 activation. (C) Cold competition using 100-fold molar excess of unlabeled NF-κB and AP-1 oligonucleotides (lanes 2 and 3) demonstrated the specificity of the protein/DNA binding complexes. Specificity of NF-κB binding was also determined by using antibodies to the NF-κB components p50, p65, c-Rel, and p52, resulting in supershift (lanes 4-7). (D) HUT-102 cells were treated with the indicated concentration of ritonavir for 24 hours, and cell lysates were immunoblotted for IκBα (top) and phospho-IκBα (middle). Actin immunoblots confirm that similar amounts of cell extracts were analyzed (bottom). (E) Primary acute-type ATL cells treated with concentrations of ritonavir as indicated for 24 hours were evaluated for NF-κB and AP-1 activation. Where indicated, 100-fold excess amounts of competitor oligonucleotides were added to the reaction mixture (lanes 4 and 5). (F) The bands of phosphorylated IκBα were down-regulated by ritonavir treatment. Detection of actin expression was used as an internal control.

type. However, AP-1 binding was not inhibited. Ritonavir abolished proximal signaling events leading to IκBα phosphorylation (Figure 2F). Twenty micromolar concentration of ritonavir caused only a partial decrease of the slower-migrating form of phosphorylated IκBα, whereas significant decrease of the slower-migrating form of phosphorylated IκBα and an accumulation of unphosphorylated IκBα were observed at 30 μM (top). Thirty micromolar concentration of ritonavir abolished the phosphorylated IκBα content (middle). We obtained similar results using another acute-type ATL cells (data not shown).

Ritonavir represses Tax-induced and constitutive transcriptional activity of NF-κB

We examined whether ritonavir inhibits the transcriptional activity of NF-κB. First, we tested the effect of ritonavir on Tax-induced NF-κB transcriptional activity in Jurkat cells (HTLV-I–uninfected cell line) transfected with Tax expression plasmid. Ritonavir caused only a partial inhibition of proliferation in Jurkat cells cultured for 24 hours even at the highest dose. Tax-induced NF-κB transcriptional activation was suppressed by ritonavir in a dose-dependent manner (Figure 3A). Next, we determined the effect of ritonavir on constitutively activated NF-κB and AP-1 transcriptional activity in an HTLV-I–infected cell line HUT-102. Ritonavir inhibited the constitutively activated transcriptional activity of NF-κB in a dose-dependent manner, but not that of AP-1 (Figure 3B). Twenty micromolar concentration of ritonavir caused only a partial inhibition of NF-κB/DNA binding (Figure 2B), whereas strong inhibition of NF-κB transcriptional activity was observed at the concentration less than 20 μM. This discrepancy might derive from differences in sensitivity between these 2 assays. These results indicate that ritonavir inhibits both Tax-induced and constitutive NF-κB transcriptional activity.

Ritonavir down-regulates the expression of NF-κB–regulated gene products

The antiproliferative and proapoptotic effects of ritonavir were explored by examining the level of intracellular regulators of cell cycle and apoptosis after exposure to ritonavir (Figure 3C). Ritonavir down-regulated levels of Bcl-X_L, survivin, cIAP2, c-Myc, cyclin D2, regulated by NF-κB,[47-51] and the phosphorylated form of pRb in HUT-102 cells cultured with 40 μM ritonavir for 72 hours. Thirty micromolar concentration of ritonavir caused only a partial down-regulation of Bcl-X_L and the phosphorylated form of pRb, whereas significant down-regulation of survivin was observed in HUT-102 cells cultured for 72 hours, suggesting that NF-κB–regulated genes have the differential sensitivity to ritonavir. However, ritonavir did not modulate levels of Bcl-2 and Tax proteins in these cells (Figure 3C; data not shown). We also explored the effect of ritonavir on NF-κB–regulated gene products in ATL cells freshly isolated from an acute-type patient. As shown in Figure 3D, Bcl-X_L, survivin, cyclin D2, and c-Myc, but not Bcl-2, showed a decline. Thus, expression of NF-κB regulated genes, the induction of which are involved in antiapoptosis (Bcl-X_L, survivin, and cIAP2) and cell cycle (cyclin D2 and c-Myc), apparently had been down-regulated in the presence of ritonavir. We obtained a similar result using other acute-type ATL

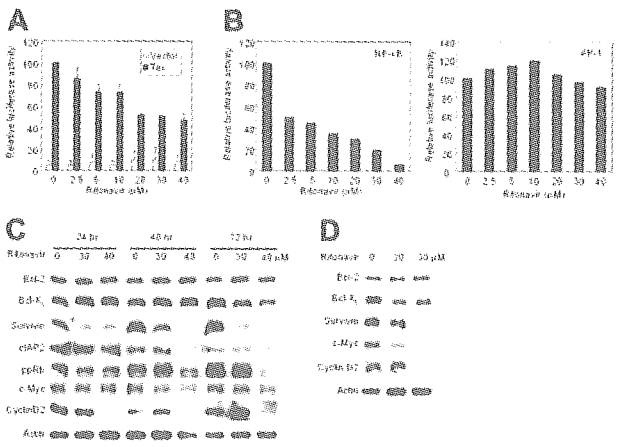

Figure 3. Ritonavir inhibits NF-κB transcriptional activation and expression of apoptosis- and cell-cycle–associated proteins. (A) Ritonavir inhibits Tax-induced NF-κB transcriptional activation. κB-LUC was transfected into Jurkat cells with Tax-expressing plasmid (▩) or empty vector (□). After transfection, cells were treated with increasing concentrations of ritonavir. Luciferase activity is expressed relative to the basal level measured in cells transfected with the reporter plasmid and Tax-expressing plasmid without further treatment, which was defined as 100. Data represent the mean + SD from 3 independent experiments. (B) Ritonavir inhibits constitutive active NF-κB transcriptional activity in HUT-102 cells. κB-LUC and AP-1–LUC were transfected into HUT-102 cells. After transfection, cells were treated as in panel A. Luciferase activity was normalized, based on the Renilla luciferase activity from phRL-TK. Relative luciferase activity is expressed relative to the basal level measured in cells transfected with the reporter plasmid without further treatment, which was defined as 100. (C-D) Western blot analyses. HUT-102 cells (C) and primary acute-type ATL cells (D) were cultured with the indicated concentration of ritonavir for 24 to 72 hours (HUT-102 cells) and 24 hours (ATL cells). Cells were harvested and subjected to Western blot analysis. The polyvinylidene fluoride membrane was sequentially probed with indicated antibodies.

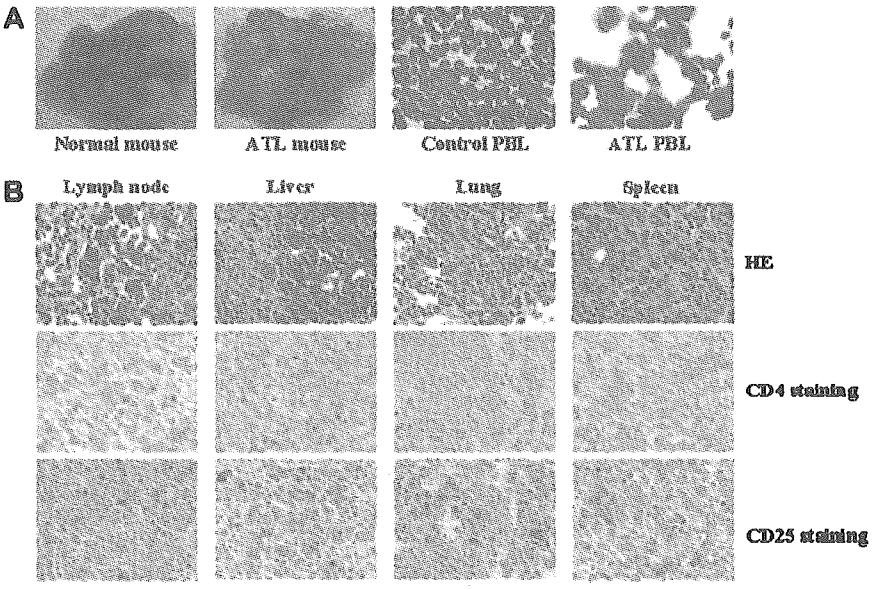

Figure 4. Successful engraftment and massive infiltration of primary ATL cells into various organs of NOG mice inoculated with PBMCs from patients with ATL. (A) Photographs of whole organs of normal and ATL cell–challenged mice with enlarged spleen, liver, and lungs (left 2 panels). Right 2 panels show May-Grunwald and Giemsa staining of PBMCs collected from normal and ATL cell–challenged mice, 2 months after inoculation of ATL cells, respectively. (B) HE (top) and immunohistochemical staining of various organs of NOG mice inoculated with ATL cells. Immunohistochemical staining using anti-CD4 (middle) and anti-CD25 (bottom) was conducted on various organs of mice tissues 2 months after inoculation of ATL cells. Magnification ×40.

cells (data not shown). Taken together these data suggest that constitutively high NF-κB activity in ATL cells is indispensable for their survival, and that specific inhibition of this activity by a clinically available drug results in the induction of apoptosis.

Establishment of a novel ATL model

PBMCs from patients with ATL were inoculated either intraperitoneally into the abdominal region or subcutaneously in the postauricular region of unconditional NOD/SCID/γc^{null} (NOG) mice. All mice developed clinical sign of near-death, such as piloerection, weight loss, and cachexia 6 to 8 weeks after inoculation of ATL cells in addition to the enlargement of lymph nodes, spleen, lungs, and liver, whereas no tumors were found in the postauricular region or abdominal cavity where primary ATL cells were inoculated (Figure 4A). There was no difference in respect to the successful engraftment of ATL cells inoculated either intraperitoneally or subcutaneously in NOG mice. Histologic analysis of ATL-bearing mice showed massive infiltration of leukemic cells in various organs of NOG mice that were efficiently expressing human CD4 and CD25 molecules (Figure 4B). A higher level of IL-2Rα (CD25) expression was observed on the surface of malignant cells associated with all stages of ATL[12-14] as well as ATL cells infiltrated into various organs of patients.[52,53] Thus, results from this model indicated successful engraftment and massive infiltration of primary ATL cells in various organs of NOG mice, like leukemia but without producing tumors at the sites of inoculation.

Ritonavir inhibits ATL cell growth and infiltration in NOG mice

To study the effect of ritonavir on ATL, we injected primary ATL cells (2×10^7) from 10 patients subcutaneously into the postauricular region of NOG mice. One day after inoculation, mice were treated with either RPMI-1640 (as control) or ritonavir (30 mg/kg/d) intraperitoneally daily for 30 days followed by observation for another 30 days without any treatment. ATL cell inoculation promoted the development of piloerection, weight loss, and cachexia, all of which are signs of near-death, in addition to the enlargement of lymph nodes, spleen, lungs, and liver in all control mice 2 months after inoculation (Figure 5A). In contrast, ritonavir-treated mice appeared to be healthy and had almost no enlargement of these organs (Figure 5A). Clinical evaluation of organ invasion 2 months after injection of primary ATL cells showed that ritonavir treatment inhibited their infiltration into lymph nodes, spleen, lungs, and liver (Figure 5B-D). Samples from 7 patients of 10 injected in mice treated with ritonavir presented substantial inhibition of organ invasion, and 2 (patients 5 and 7) showed partial inhibition, whereas one sample (patient 6) failed to do so (Table 2).

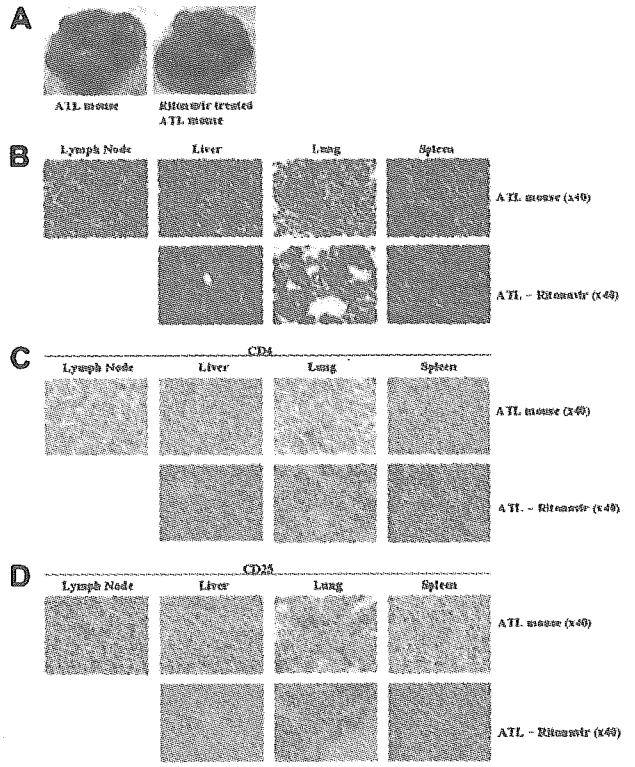

Figure 5. Effect of ritonavir on ATL cell growth and infiltration. (A) Mice were injected with ATL cells (2×10^7 cells) subcutaneously in the postauricular region. One day after inoculation, the mice were administered either RPMI 1640 or ritonavir (30 mg/kg/d) intraperitoneally every day for 30 days followed by observation for another month without therapy. Photographs of whole organs of RPMI 1640–treated ATL mice (left) and ritonavir-treated ATL mice (right) with enlarged spleen, liver, and lungs. (B-D) HE staining (B) and immunohistochemical staining using anti-CD4 (C) or anti-CD25 (D) in various organs of NOG mice 2 months after inoculation of ATL cells. Upper panels show various organs of mice treated with RPMI 1640, and lower panels represent various organs of mice treated with ritonavir. Magnification ×40.

Table 2. Effect of ritonavir on infiltration of ATL cells in various organs of SCID mice

Patient no. and treatment	Liver	Spleen	Lung	Lymph node
1				
Control	+++	+++	+++	+++
Ritonavir	++	+	+	NF
2				
Control	+++	+++	++	+++
Ritonavir	+	+	−	NF
3				
Control	+++	+++	+++	+++
Ritonavir	±	±	±	NF
4				
Control	+++	+++	+++	+++
Ritonavir	+	+	+	NF
5				
Control	+++	+++	+++	+++
Ritonavir	++	++	++	NF
6				
Control	+++	+++	+++	+++
Ritonavir	+++	++	+++	++
7				
Control	+++	+++	+++	+++
Ritonavir	++	+	++	NF
8				
Control	+++	+++	+++	+++
Ritonavir	±	±	±	NF
9				
Control	+++	+++	+++	++
Ritonavir	++	+	+	NF
10				
Control	+++	+++	++	+++
Ritonavir	+	+	+	NF

PBMCs from patients with ATL patients were inoculated subcutaneously into postauricular region of NOG mice, which were treated with ritonavir or RPMI-1640 as a control 1 day after inoculation for 1 month. Various organ infiltration was evaluated 2 months after inoculation.

NF indicates no formation of new lymph node; +++, massive; ++, marked; +, slight; ±, focally present or no infiltration; −, no infiltration.

In contrast, all control mice showed formation of new lymph nodes and infiltration with ATL cells into various organs (Figure 5B-D; Table 2). Organ infiltration of primary ATL cells was analyzed and evaluated by HE staining and immunostaining of CD4 and CD25. Together, these data indicate that ritonavir significantly inhibits ATL cell growth and infiltration in various organs of NOG mice (Figure 5).

Discussion

ATL is a malignancy of $CD4^+$ T-lymphocytes etiologically linked to a retrovirus, HTLV-I.[1-3] The malignant cells associated with all phases of ATL express very high levels of IL-2Rα (CD25).[12-14] The median survival duration of all patients with aggressive ATL was 13 months, and overall survival at 2 years was estimated to be 31.3%.[6] The various chemotherapies so far developed have not increased significantly the survival of patients with ATL. Given disappointing results using conventional chemotherapy, new approaches for the treatment of ATL are required. Previous reports have shown that primary ATL cells proliferate and infiltrate into various organs of SCID mice.[54-56] Our ATL model was consistent with others, but it represented more aggressive features about cell growth and infiltration in SCID mice. The tumor cells massively infiltrated into various organs in a manner similar to a leukemia-expressing T-cell marker CD4 and an activating marker CD25, especially into the spleen, lymph nodes, liver, and lungs of NOG mice. Our NOG ATL model presents many features 6 to 8 weeks after inoculation of ATL cells such as the clinical signs observed in patients with ATL. Two clinical types, acute and chronic, carry very different prognosis. However, no difference of cell growth, surface phenotype, and NF-κB activity is observed in primary leukemic cells from patients with acute- and chronic-type ATL. Therefore, the same characteristics of freshly isolated ATL cells with acute- and chronic-type were observed in NOG mice. Thus, it represents a novel model to evaluate tissue toxicity and the efficacy of therapeutic agents directed toward the treatment of ATL.

Constitutive NF-κB activation was demonstrated not only in HTLV-I–infected cell lines but also on fresh ATL cells regardless of Tax expression,[15] which could contribute to the drug-resistance of ATL cells through overexpression of Bcl-X_L.[51] We and others have previously reported that suppression of high NF-κB activity inhibited cell growth and induced apoptosis of HTLV-I–infected cell lines and primary ATL cells both in vitro and in vivo.[21-24] Recently, ritonavir has been shown to inhibit NF-κB activity induced by activators such as TNFα, Tat, and ORF74.[34] This led us to investigate whether this drug exhibits anti-ATL effects in vitro and in our preclinical murine ATL model. In the present study, we revealed that ritonavir treatment of HTLV-I–infected cell lines and ATL cells inhibited phosphorylation of IκBα, allowing suppression of NF-κB activity. Our results also suggest that inhibition of NF-κB activity by ritonavir reduced cell growth and induced apoptosis of these cells. This is consistent with down-modulation of NF-κB–regulated genes such as antiapoptotic (Bcl-X_L,[50,51] cIAP2,[57] and survivin[49]) and cell-cycle–related (cyclin D2[48] and c-Myc[47]) genes. We also examined the effect of ritonavir on the proliferation of an HTLV-I–negative T-cell line, Jurkat, in vitro. Exposure of ritonavir for 72 hours reduced the rate of proliferation (data not shown). Because ritonavir is suggested to affect proteasomal proteolysis,[33] it may effect a stabilization of p21, p27, and p53 proteins. Like proteasome inhibitors, ritonavir may also affect multiple pathways critical for survival of HTLV-I–positive and –negative malignant T cells. Additional experiments will be necessary to elucidate the mechanisms of anti-ATL activity.

In the therapy of HIV infection, the blood plasma ritonavir concentrations are between 5 and 15 μM,[58] but much higher maximal concentrations (up to 46 μM) have been determined in individual patients.[59] In the present study, we used the concentration of ritonavir for doing in vitro experiments from 0 to 40 μM and in vivo 30 mg/kg/d used for treatment of patients with AIDS. Our murine ATL model clearly indicates that 30 mg/kg/d of ritonavir significantly inhibits ATL cell growth and infiltration into various organs of NOG mice. The plasma exposure produced by this dose in mice is only approximately one half of the plasma exposure observed with the licensed dose of ritonavir in humans (600 mg twice daily). In our NOG ATL model, ritonavir at this treatment dosage is well tolerated without severe adverse effects observed in the mice during the treatment period. These data strongly suggest that the HIV PI, ritonavir, is a promising antitumor agent against ATL and could be used clinically for ATL regimens. Ritonavir exhibited anti-ATL activity against leukemic cells from patients

with acute- and chronic-type ATL in vitro and in vivo. The expression of CD25 and NF-κB activity do not differ between acute and chronic ATL cells.[12-15] These results suggest that anti-ATL activity of ritonavir correlates with suppression of NF-κB activity. It is also of interest to note that HTLV-I uses an aspartic protease analogous to HIV protease in its replication. To our knowledge, the activity of ritonavir against HTLV-I protease has not been assessed. Although Tax expression is very low or undetectable in ATL malignancy, a direct antiviral effect of ritonavir cannot be ruled out at this time.

In summary, using a large number of patient samples we have established a novel NOG ATL model that presents features similar to patients with ATL. These results also indicate that the HIV PI, ritonavir, showed antitumor and anti–NF-κB activity against primary ATL cells. Finally, our results strongly suggest that NF-κB serves as a potential molecular target to treat ATL, and that ritonavir might be used clinically as a single compound or in combination with the reducing dose of chemotherapeutic agents for treatment of patients with ATL.

Acknowledgments

We thank D. Kempf and T. Yamada of Abbott Laboratories, N. Yamamoto and S. Takeda of Molecular Virology, S. Ichinose of the Instrumental Analysis Research Center, S. Endo of the Animal Research Center, Tokyo Medical and Dental University, and P.J. Richard of Cardiff University for their advice and assistance with the experiments, and Y. Sato of the National Institute of Infectious Diseases for her excellent technical assistance. We thank J. Fujisawa for providing a luciferase reporter construct, κB-LUC, K. Matsumoto for providing the Tax expression plasmid, M. Maeda for providing ED-40 515(−), and the Fujisaki Cell Center, Hayashibara Biomedical Laboratories, for providing the MT-1, HUT-102, and C5/MJ cell lines.

References

1. Hinuma Y, Nagata K, Hanaoka M, et al. Adult T-cell leukemia: antigen in an ATL cell line and detection of antibodies to the antigen in human sera. Proc Natl Acad Sci U S A. 1981;78:6476-6480.
2. Poiesz BJ, Ruscetti FW, Gazdar AF, Bunn PA, Minna JD, Gallo RC. Detection and isolation of type C retrovirus particles from fresh and cultured lymphocytes of a patient with cutaneous T-cell lymphoma. Proc Natl Acad Sci U S A. 1980;77:7415-7419.
3. Yoshida M, Miyoshi I, Hinuma Y. Isolation and characterization of retrovirus from cell lines of human adult T-cell leukemia and its implication in the disease. Proc Natl Acad Sci U S A. 1982;79:2031-2035.
4. Takatsuki K, Uchiyama T, Sagawa K, Yodoi J. Adult T-cell leukemia in Japan. In: Seno S, Takaku F, Irino S, eds. Topics in Hematology. Amsterdam, The Netherlands: Excerpta Medica; 1977:73-77.
5. Uchiyama T, Yodoi J, Sagawa K, Takatsuki K, Uchino H. Adult T-cell leukemia: clinical and hematologic features of 16 cases. Blood. 1977;50:481-492.
6. Yamada Y, Tomonaga M, Fukuda H, et al. A new G-CSF-supported combination chemotherapy, LSG15, for adult T-cell leukaemia-lymphoma: Japan Clinical Oncology Group Study 9303. Br J Haematol. 2001;113:375-382.
7. Felber BK, Paskalis H, Kleinman-Ewing C, Wong-Staal F, Pavlakis GN. The pX protein of HTLV-I is a transcriptional activator of its long terminal repeats. Science. 1985;229:675-679.
8. Sodroski JG, Rosen CA, Haseltine WA. Trans-acting transcriptional activation of the long terminal repeat of human T lymphotropic viruses in infected cells. Science. 1984;225:381-385.
9. Maruyama M, Shibuya H, Harada H, et al. Evidence for aberrant activation of the interleukin-2 autocrine loop by HTLV-1-encoded p40x and T3/Ti complex triggering. Cell. 1987;48:343-350.
10. Ballard DW, Bohnlein E, Lowenthal JW, Wano Y, Franza BR, Greene WC. HTLV-I tax induces cellular proteins that activate the κB element in the IL-2 receptor α gene. Science. 1988;241:1652-1655.
11. Cross SL, Feinberg MB, Wolf JB, Holbrook NJ, Wong-Staal F, Leonard WJ Regulation of the human interleukin-2 receptor α chain promoter: activation of a nonfunctional promoter by the transactivator gene of HTLV-I. Cell. 1987;49:47-56.
12. Uchiyama T, Broder S, Waldmann TA. A monoclonal antibody (anti-Tac) reactive with activated and functionally mature human T cells, I: production of anti-Tac monoclonal antibody and distribution of Tac (+) cells. J Immunol. 1981;126:1393-1397.
13. Uchiyama T, Hori T, Tsudo M, et al. Interleukin-2 receptor (Tac antigen) expressed on adult T cell leukemia cells. J Clin Invest. 1985;76:446-453.
14. Waldmann TA, Greene WC, Sarin PS, et al. Functional and phenotypic comparison of human T cell leukemia/lymphoma virus positive adult T cell leukemia with human T cell leukemia/lymphoma virus negative Sezary leukemia, and their distinction using anti-Tac. Monoclonal antibody identifying the human receptor for T cell growth factor. J Clin Invest. 1984;73:1711-1718.
15. Mori N, Fujii M, Ikeda S, et al. Constitutive activation of NF-κB in primary adult T-cell leukemia cells. Blood. 1999;93:2360-2368.
16. Baldwin AS. The NF-κB and IκB proteins: new discoveries and insights. Annu Rev Immunol. 1999;14:649-681.
17. Watanabe M, Dewan MZ, Okamura T, et al. A novel NF-κB inhibitor DHMEQ selectively targets constitutive NF-κB activity and induces apoptosis of multiple myeloma cells in vitro and in vivo. Int J Cancer. 2005;114:32-38.
18. Adams J, Palombella VJ, Elliott PJ. Proteasome inhibition: a new strategy in cancer treatment. Invest New Drugs. 2000;18:109-121.
19. Teicher BA, Ara G, Herbst R, Palombella VJ, Adams J. The proteasome inhibitor PS-341 in cancer therapy. Clin Cancer Res. 1999;5:2638-2645.
20. Hideshima T, Chauhan D, Richardson P, et al. NF-κB as a therapeutic target in multiple myeloma. J Biol Chem. 2002;277:16639-16647.
21. Dewan MZ, Terashima K, Taruishi M, et al. Rapid tumor formation of human T-cell leukemia virus type 1-infected cell lines in novel NOD-SCID/γc^{null} mice: suppression by an inhibitor against NF-κB. J Virol. 2003;77:5286-5294.
22. Kitajima I, Shinohara T, Bilakovics J, Brown DA, Xu X, Nerenberg M. Ablation of transplanted HTLV-I Tax-transformed tumors in mice by antisense inhibition of NF-κB. Science. 1992;258:1792-1795.
23. Mori N, Yamada Y, Ikeda S, et al. Bay 11-7082 inhibits transcription factor NF-κB and induces apoptosis of HTLV-I–infected T-cell lines and primary adult T-cell leukemia cells. Blood. 2002;100:1828-1834.
24. Tan C, Waldmann TA. Proteasome inhibitor PS-341, a potential therapeutic agent for adult T-cell leukemia. Cancer Res. 2002;62:1083-1086.
25. Collier AC. Efficacy of combination antiretroviral therapy. Adv Exp Med Biol. 1996;394:355-372.
26. Collier AC, Coombs RW, Schoenfeld DA, Bassett R, Baruch A, Corey L. Combination therapy with zidovudine, didanosine and saquinavir. Antiviral Res. 1996;29:99.
27. Collier AC, Coombs RW, Schoenfeld DA, et al. Treatment of human immunodeficiency virus infection with saquinavir, zidovudine, and zalcitabine. AIDS Clinical Trials Group. N Engl J Med. 1996;334:1011-1017.
28. Markowitz M, Saag M, Powderly WG, et al. A preliminary study of ritonavir, an inhibitor of HIV-1 protease, to treat HIV-1 infection. N Engl J Med. 1995;333:1534-1539.
29. Kempf DJ, Marsh KC, Denissen JF, et al. ABT-538 is a potent inhibitor of human immunodeficiency virus protease and has high oral bioavailability in humans. Proc Natl Acad Sci U S A. 1995;92:2484-2488.
30. Andre P, Groettrup M, Klenerman P, et al. An inhibitor of HIV-1 protease modulates proteasome activity, antigen presentation, and T cell responses. Proc Natl Acad Sci U S A. 1998;95:13120-13124.
31. Liang JS, Distler O, Cooper DA, Jamil H, Deckelbaum RJ, Ginsberg HN, Sturley SL. HIV protease inhibitors protect apolipoprotein B from degradation by the proteasome: a potential mechanism for protease inhibitor-induced hyperlipidemia. Nat Med. 2001;7:1327-1331.
32. Schmidtke G, Holzhutter HG, Bogyo M, et al. How an inhibitor of the HIV-I protease modulates proteasome activity. J Biol Chem. 1999;274:35734-35740.
33. Gaedicke S, Firat-Geier E, Constantiniu O, et al. Antitumor effect of the human immunodeficiency virus protease inhibitor ritonavir: induction of tumor-cell apoptosis associated with perturbation of proteasomal proteolysis. Cancer Res. 2002;62:6901-6908.
34. Pati S, Pelser CB, Dufraine J, Bryant JL, Reitz MS Jr, Weichold FF. Antitumorigenic effects of HIV protease inhibitor ritonavir: inhibition of Kaposi sarcoma. Blood. 2002;99:3771-3779.
35. Sgadari C, Barillari G, Toschi E, et al. HIV protease inhibitors are potent anti-angiogenic molecules and promote regression of Kaposi sarcoma. Nat Med. 2002;8:225-232.
36. Miyoshi I, Kubonishi I, Yoshimoto S, et al. Type C virus particles in a cord T-cell line derived by cocultivating normal human cord leukocytes and

human leukaemic T cells. Nature. 1981;294:770-771.

37. Yamamoto N, Okada M, Koyanagi Y, Kannagi M, Hinuma Y. Transformation of human leukocytes by cocultivation with an adult T cell leukemia virus producer cell line. Science. 1982;217:737-739.
38. Popovic M, Sarin PS, Robert-Gurroff M, et al. Isolation and transmission of human retrovirus (human T-cell leukemia virus). Science. 1983;219:856-859.
39. Koeffler HP, Chen IS, Golde DW. Characterization of a novel HTLV-infected cell line. Blood. 1984;64:482-490.
40. Miyoshi I, Kubonishi I, Sumida M, et al. A novel T-cell line derived from adult T-cell leukemia. Gann. 1980;71:155-156.
41. Maeda M, Shimizu A, Ikuta K, et al. Origin of human T-lymphotrophic virus I-positive T cell lines in adult T cell leukemia. Analysis of T cell receptor gene rearrangement. J Exp Med. 1985;162:2169-2174.
42. Ishiyama M, Shiga M, Sasamoto K, Mizoguchi M, He P. A new sulfonated tetrazolium salt that produces a highly water-soluble formazan dye. Chem Pharm Bull. 1993;41:1118-1122.
43. Zhang C, Ao Z, Seth A, Schlossman SF. A mitochondrial membrane protein defined by a novel monoclonal antibody is preferentially detected in apoptotic cells. J Immunol. 1996;157:3980-3987.
44. Seth A, Zhang C, Letvin NL, Schlossman SF. Detection of apoptotic cells from peripheral blood of HIV-infected individuals using a novel monoclonal antibody. AIDS. 1997;11:1059-1061.
45. Matsumoto K, Shibata H, Fujisawa J, et al. Human T-cell leukemia virus type 1 Tax protein transforms rat fibroblasts via two distinct pathways. J Virol. 1997;71:4445-4451.
46. Dewan MZ, Watanabe M, Terashima K, et al. Prompt tumor formation and maintenance of constitutive NF-κB activity of multiple myeloma cells in NOD/SCID/γc^{null} mice. Cancer Sci. 2004;95:1-5.
47. Duyao MP, Kessler DJ, Spicer DB, et al. Transactivation of the c-myc promoter by human T cell leukemia virus type 1 tax is mediated by NFκB. J Biol Chem. 1992;267:16288-16291.
48. Huang Y, Ohtani K, Iwanaga R, Matsumura Y, Nakamura M. Direct trans-activation of the human cyclin D2 gene by the oncogene product Tax of human T-cell leukemia virus type I. Oncogene. 2001;20:1094-1102.
49. Mitsiades N, Mitsiades CS, Poulaki V, et al. Biologic sequelae of nuclear factor-κB blockade in multiple myeloma: therapeutic applications. Blood. 2002;99:4079-4086.
50. Mori N, Fujii M, Cheng G, et al. Human T-cell leukemia virus type I tax protein induces the expression of anti-apoptotic gene Bcl-x_L in human T-cells through nuclear factor-κB and c-AMP responsive element binding protein pathways. Virus Genes. 2001;22:279-287.
51. Nicot C, Mahieux R, Takemoto S, Franchini G. Bcl-X_L is up-regulated by HTLV-I and HTLV-II in vitro and in ex vivo ATLL samples. Blood. 2000;96:275-281.
52. Tamura K. Clinical classification of adult T-cell leukemia and its complications. Rinsho Byori. 1996;44:19-23.
53. Watanabe T. HTLV-1-associated diseases. Int J Hematol. 1997;66:257-278.
54. Imada K, Takaori-Kondo A, Sawada H, et al. Serial transplantation of adult T cell leukemia cells into severe combined immunodeficient mice. Jpn J Cancer Res. 1996;87:887-892.
55. Kondo A, Imada K, Hattori T, et al. A model of in vivo cell proliferation of adult T-cell leukemia. Blood. 1993;82:2501-2509.
56. Phillips KE, Herring B, Wilson LA, et al. IL-2Rα-directed monoclonal antibodies provide effective therapy in a murine model of adult T-cell leukemia by a mechanism other than blockade of IL-2/IL-2Rα interaction. Cancer Res. 2000;60:6977-6984.
57. Chu ZL, McKinsey TA, Liu L, Gentry JJ, Malim MH, Ballard DW. Suppression of tumor necrosis factor-induced cell death by inhibitor of apoptosis c-IAP2 is under NF-κB control. Proc Natl Acad Sci U S A. 1997;94:10057-10062.
58. Norvir, ritonavir product monograph. North Chicago, IL: Abbott Laboratories, 1997.
59. Gatti G, Di Biagio A, Casazza R, et al. The relationship between ritonavir plasma levels and side-effects: implications for therapeutic drug monitoring. AIDS. 1999;13:2083-2089.

Virchows Arch (2005) 447: 53–60
DOI 10.1007/s00428-005-1275-6

ORIGINAL ARTICLE

Naoya Nakamura · Hidenori Hase · Daisuke Sakurai · Sachiko Yoshida · Masafumi Abe · Nobuhiro Tsukada · Jun Takizawa · Sadao Aoki · Masaru Kojima · Shigeo Nakamura · Tetsuji Kobata

Expression of BAFF-R (BR3) in normal and neoplastic lymphoid tissues characterized with a newly developed monoclonal antibody

Received: 10 January 2005 / Accepted: 12 April 2005 / Published online: 14 June 2005

Abstract BAFF-receptor (BAFF-R) is required for the successful maturation and survival of B-cells. We developed an anti-human BAFF-R monoclonal antibody (mAb), 8A7. The reactivity of 8A7 in normal and neoplastic tissue was examined by performing immunohistochemistry on paraffin-embedded sections. 8A7 reacted with lymphocytes in the mantle and marginal zones, but not with lymphocytes in the interfollicular area. Lymphocytes in the germinal centers were found to be negative or occasionally weakly positive for 8A7. BAFF-R expression was found only in B-cell lymphoma (44/80, positive cases/examined cases): B-lymphoblastic lymphoma 0/3, B-chronic lymphocytic leukemia/small lymphocytic lymphoma 4/4, mantle cell lymphoma 9/11, follicular lymphoma 10/14, diffuse large B-cell lymphoma (DLBCL) 11/25, marginal zone B-cell lymphoma 8/10, lymphoplasmacytic lymphoma 2/2, plasma cell myeloma 0/2, and Burkitt lymphoma 0/9, but not in T/NK cell lymphomas (0/19) or Hodgkin lymphoma (0/10). BAFF-R was expressed in most low-grade B-cell neoplasms and a small number of DLBCL, suggesting that BAFF-R may play an important role in the proliferation of neoplastic lymphoid cells. Thus, the mAb is very useful for further understanding of both healthy B-cell biology and its pathogenic neoplasms.

Keywords BAFF · BAFF-R · Monoclonal antibody · Immunohistochemistry · B-cell lymphoma · Diffuse large B-cell lymphoma

N. Nakamura (✉) · S. Yoshida · M. Abe
Department of Pathology,
Fukushima Medical University,
Hikarigaoka-1,
Fukushima-shi, 960-1295, Japan
e-mail: nao@fmu.ac.jp
Tel.: +81-24-5484488
Fax: +81-24-5484488

H. Hase · D. Sakurai · T. Kobata
Department of Immunology,
Dokkyo University School of Medicine,
Tochigi, Japan

N. Tsukada · J. Takizawa · S. Aoki
First Department of Internal Medicine,
Niigata University Medical Hospital,
Niigata University,
Niigata, Japan

M. Kojima
Department of Pathology,
Dokkyo University School of Medicine,
Tochigi, Japan

S. Nakamura
Department of Pathology and Molecular Diagnostics,
Aichi Cancer Center,
Nagoya, Japan

Introduction

B-cell-activating factor of the tumor necrosis factor (TNF) family (BAFF), also known as BLyS, THANK, TALL-1 and zTNF4, is a fundamental survival factor for B-cells, and BAFF functionality is indispensable for B-cell maturation [13, 18, 27, 28]. BAFF is a trimeric membrane-bound or soluble factor and is expressed by monocytes, macrophages, neutrophils and dendritic cells. Whereas BAFF-deficient mice lack mature B-cells, BAFF-transgenic mice, characterized by overexpression of BAFF, have increased the number of B-cells and develop autoimmunity [3, 4, 9, 12]. In particular, transitional type 2 (T2) B-cells and marginal zone B-cells are expanded in BAFF-transgenic mice. BAFF blockade does not inhibit germinal center (GC) formation or somatic hypermutation of immunoglobulin (Ig) genes, indicating that BAFF is required for the normal maintenance of B-cells, but not for the initiation of the GC reaction, although B-cell maturation and mature functions are severely impaired [35]. Recently, it was reported that BAFF is directly involved in B cell malignancy [2, 7, 22, 23].

Three receptors for BAFF have been established: B-cell maturation antigen (BCMA), transmembrane activator and

calcium-modulator, and cyclophilin ligand interactor (TA CI) and the BAFF-receptor (BAFF-R, also called BR3) [3, 14, 32, 33]. All three receptors are expressed on B-cells, while TACI is also expressed on activated T-cells [13]. Whereas TACI and BCMA are found to bind to a proliferation-inducing ligand (APRIL), BAFF-R binds only to BAFF [13, 32]. TACI is known to negatively control B-cell homeostasis and T-cell independent immune responses from evidence obtained from TACI deficient mice [30, 34, 37]. Although BCMA was recently reported to be essential for the survival of plasma cells [1, 24], mice lacking BC MA possess normal-appearing B lymphocyte compartments [27]. Thus, only BAFF-R is clearly a key receptor involved in the successful survival and maturation of B-cells [13]. However, the distribution of BAFF-R in normal and malignant human lymphoid tissue has not been made fully clear.

Only a few reports on BAFF-R in malignant B-cells have appeared to date. Briones et al. examined the BAFF binding activity in 43 cases of non-Hodgkin's lymphoma (NHL) with flow cytometry [2]. Although all cases of NHL express receptors for BAFF, BAFF-R expression was not specifically classified. Chronic lymphocytic leukemia/small lymphocytic lymphoma (CLL/SLL), mantle cell lymphoma (MCL), follicular center lymphoma, Burkitt lymphoma (BL) and diffuse large cell lymphoma were reported to express BAFF-R mRNA [7, 22], and multiple myeloma (MM) was reported to express cell surface BAFF-R [23].

In this investigation, we established the mouse anti-human BAFF-R monoclonal antibody (mAb) and examined its reactivity in normal and neoplastic lymphoid tissues using immunohistochemistry. We found a high degree of significance in its distribution in normal lymphoid tissue and low-grade B-cell neoplasms as well as in a small part of diffuse large B-cell lymphoma (DLBCL).

Materials and methods

Cell preparation and cell cultures

Human peripheral blood mononuclear cells were isolated from pooled healthy donors by Ficoll-Hypaque density-gradient centrifugation. After the depletion of monocytes by adherence to the plastic surface of the culture dishes, E rosette-negative populations were collected with 5% sheep erythrocytes and Ficoll-Hypaque. Purified B-cells were isolated by depleting the non B-cells using a B-cell isolation kit and auto MACS (Miltenyi Biotec, Auburn, Calif., USA). The resultant B-cell population was <2% $CD14^+$, <1% $CD3^+$, <2% $CD57^+$, and >95% $CD20^+$. All cultures were conducted in RPMI 1640 medium supplemented with 25 mM HEPES (*N*-2-hydroxyethylpiperazine-*N'*-2-ethanesulfonic acid), 10% fetal calf serum, 2 mM L-glutamine, 1 mM sodium pyruvate, 5.5×10^{-2} mM 2-mercaptoethanol, 100 IU/ml penicillin, and 100 IU/ml streptomycin (all from Invitrogen, Carlsbad, Calif., USA).

Antibodies and reagents

Polyclonal anti-human BAFF-R antibody (C-20), control mouse IgG2a, and FITC-labeled goat antibody to mouse IgG were purchased from Santa Cruz Biotechnology (Santa Cruz, Calif., USA), Sigma-Aldrich (St Louis, Mo., USA), and CALTAG (Burlingame, Calif., USA), respectively.

Establishment of human BAFF-R transfectant

To construct a human BAFF-R expression vector, a cDNA encoding full-length human BAFF-R protein (GenBank No. AF373846) was custom-synthesized (Takara, Shiga, Japan), inserted into pBluescript SK (+) (Stratagene, La Jolla, Calif., USA) at the *Eco*RI and *Bam*HI sites, and finally into the pBCMGSneo expression vector [8] at the *Xho*I and *Not*I sites (pBCMGS-BAFF-R). Murine pre-B-cells (cell line 300-19) were electroporated with pBCMGS-BAFF-R and stable transfectants were selected with G418 treatment. Cells with high-density BAFF-R were cloned with a fluorescence-activated cell sorter (FACS). The vector alone-transfected cells (mock) have been described previously [6].

Generation of anti-human BAFF-R mAb

A BALB/c mouse was immunized with human BAFF-R-expressing transfectant cells 3 times at 10-day intervals. Three days after the final immunization, the splenocytes were fused with NS-1 cells (purchased from Human Science Research Resources Bank), and HAT (hypoxanthine-aminopterin-thymidine) selection and cloning of hybridomas were performed simultaneously using a hybridoma cloning kit (ClonaCell-HY; StemCell Technologies, British Columbia, Canada). Anti-human BAFF-R designated 8A7 (mouse IgG2a, κ) was established.

Immunoblot analysis

PBS-washed cell pellets were resuspended with 0.5% SDS solution and boiled for 5 min. Proteins (5–8 μg) were separated with SDS-PAGE, transferred to an Immobilon-P membrane (Millipore, Billerica, Mass., USA), blocked with 5% skim milk, and immunoblotted with arbitrary Ab and HRP-labeled secondary Ab. The immunoblots were developed by using the enhanced chemiluminescent substrate (SuperSignal West Pico; Pierce Chemical Co., Rockford, Ill., USA) and visualized with a LumiVision analyzer (Taitec Co., Tokyo), as previously described [5].

Flow cytometric analysis

Flow cytometric analysis was performed using FACScalibur and the associated Cell Quest software (both from Becton Dickinson, San Jose, Calif., USA). FITC-labeled

goat antibody to mouse IgG was used as a second Ab. An isotype-matched mouse IgG2a control was used throughout the studies and always reacted with <5% of the cells.

Tissues and immunohistochemistry

Formalin-fixed paraffin-embedded tissues were used in this study. Tonsils resected due to chronic tonsillitis, lymph nodes resected due to non-neoplastic lymphadenopathy, spleens resected because of non-lymphoma and bone marrow clots without malignancy were used for the non-neoplastic lymphoid tissues. Neoplastic lymphoid tissues from 109 cases were used in this study and comprised the following: three cases of B-lymphoblastic lymphoma (B-LBL), four cases of CLL/SLL, 11 cases of MCL, 14 cases of follicular lymphoma (FL), 25 cases of DLBCL, ten cases of marginal zone B-cell lymphoma (MZBCL), two cases of Lymphoplasmacytic lymphoma (LPL), two cases of plasma cell myeloma (PCM), nine cases of BL, three cases of T-lymphoblastic lymphoma, four cases of angioimmunoblastic T-cell lymphoma, five cases of peripheral T-cell lymphoma, unspecified, two cases of adult T-cell lymphoma, one case of systemic anaplastic large cell lymphoma, four cases of NK/T cell lymphoma and ten cases of Hodgkin lymphoma (HL). All cases of CLL/SLL and MCL expressed CD5. Cyclin D1 was immunohistochemically detected in all but one case of MCL. FL consisted of four cases of grade 1, four cases of grade 2 and six cases of grade 3. All cases of FL expressed CD10. DLBCL included three cases with CD5 (+) CD10 (−), three cases with CD5 (−) CD10 (+) and 19 cases with CD5 (−) CD10 (−). HL consisted of three cases of nodular lymphocyte predominance Hodgkin lymphoma (NLP-HL), four cases of mixed cellularity classical Hodgkin lymphoma (MC-CHL) and three cases of nodular sclerosis classical Hodgkin lymphoma (NS-CHL).

The de-paraffinized tissue section was pre-treated in citrate buffer with microwave oven heating. The section was incubated with the primary antibody at 4°C overnight and then the streptavidin-biotin complex method (Dakocytomation, Kyoto, Japan) was used. Neoplasms with >10% positive cells were judged as positive.

Results

Establishment of the anti-human BAFF-R mAb, 8A7

To evaluate the role of the interactions between BAFF and BAFF-R in human B cell responses, we developed an anti-human BAFF-R mAb. For this purpose, we first estab-

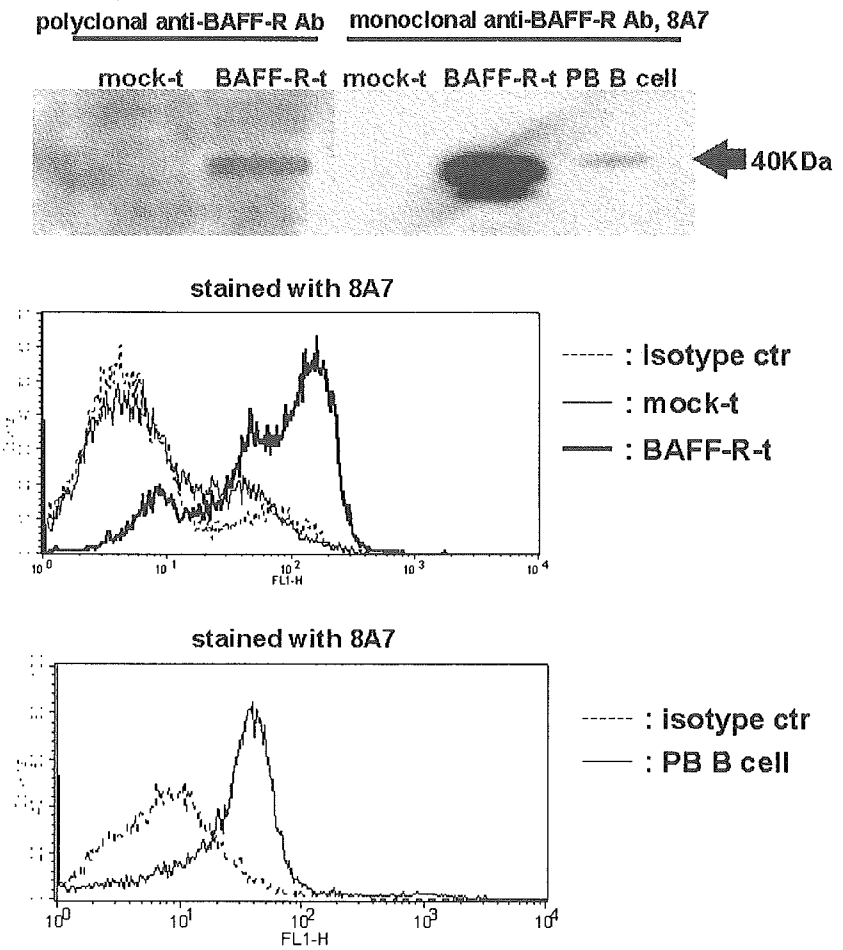

Fig. 1 8A7 mAb detects human BAFF-R. (**a**) Cell lysates prepared from BAFF-R- and mock-transfectants, and peripheral blood B cells, were subjected to immunoblot analysis using anti-human BAFF-R polyclonal Ab or 8A7 mAb. (**b**) Flow cytometric analysis of BAFF-R expression using 8A7 mAb. BAFF-R- and mock-transfectants and peripheral blood B cells were stained with 8A7 mAb or isotype-matched control Ab (IgG2a) followed by FITC-conjugated Ab to mouse IgG. Data shown are representative of three different experiments

lished a transfectant stably expressing human BAFF-R. Stable expression of human BAFF-R on the cDNA transfectant, but not on mock-transfected cells was verified using immunoblot analysis (Fig. 1a). Immunoblot analysis using commercially available polyclonal anti-human BA FF-R Ab revealed that BAFF-R cDNA-transfected cells expressed the BAFF-R molecule. We then immunized a BALB/c mouse with the BAFF-R-transfectant and fused the splenocytes with NS-1 myeloma cells. The hybridomas producing anti-human BAFF-R mAb were screened for specific reactivity to the BAFF-R-transfectant. As shown in Fig. 1a, one obtained mAb, designated 8A7, bound to BAFF-R-transfectant and peripheral blood B cells but not to mock-transfectant. Flow cytometric analysis revealed that the 8A7 mAb reacted with almost all peripheral blood B cells and BAFF-R-transfectant, but not with peripheral blood T-cells, monocytes, or mock-transfectant (Fig. 1b, data not shown).

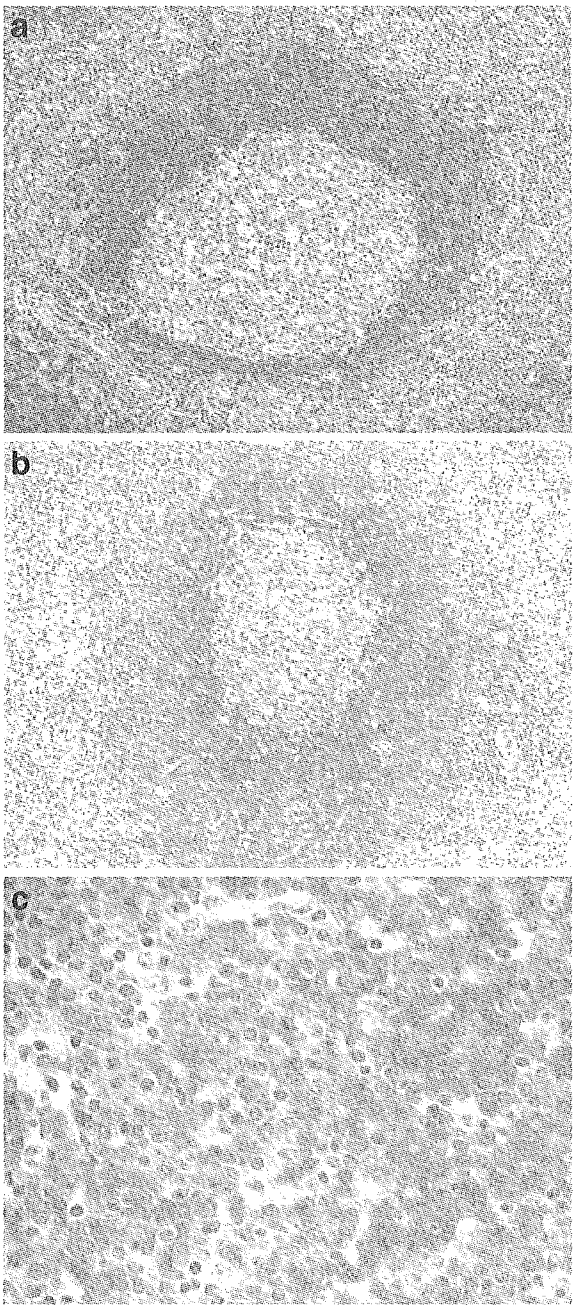

Fig. 2 BAFF-R expression in normal lymphoid tissues according to immunohistochemistry (IHC) on the paraffin-embedded section (strept/ABC method). 8A7 reacts with lymphocytes in the mantle zone of the secondary lymphoid follicles in the lymph node (**a**: IHC, original magnification ×50) and with lymphocytes in the mantle and marginal zones of the splenic white pulp (**b**: IHC, ×50). Marginal B-cells with a clear cytoplasm are positive for 8A7 (**c**: IHC, ×200)

Immunohistochemistry of non-neoplastic lymphoid tissue

8A7 reacted with lymphocytes in the mantle zone of the secondary lymphoid follicles in the tonsil (Fig. 2a) and the non-neoplastic lymph nodes. In the spleen, 8A7 reacted with lymphocytes in the mantle and marginal zones of the white pulp, but not with the interfollicular area (Fig. 2b,c). Lymphocytes in germinal centers (GCs) were found to be negative or occasionally weakly positive for hyperplastic GC. 8A7 failed to stain hematopoietic cells in the bone marrow. Plasma cells were negative for 8A7.

Immunohistochemistry of the neoplastic lymphoid tissue

Expression of BAFF-R in neoplastic lymphoid tissue detected by 8A7 is shown in Table 1 and Fig. 3. BAFF-R expression was only found in B-cell lymphoma (44/80, positive cases/examined cases), but not in T/NK cell lymphoma (0/19) or in Hodgkin lymphoma (0/10).

Discussion

An anti-human BAFF-R mAb, named 8A7, was developed using a transfectant stably expressing human BAFF-R to evaluate the role of interactions between BAFF and BAFF-R in human B-cell responses and malignancy. In this paper, reactivity and distribution in normal and malignant lymphoid tissues was addressed by means of immunohistochemistry with paraffin-embedded tissue.

The distribution of BAFF-R in human lymphoid tissue has not been heretofore reported, except in a recent report by Ng et al. [21]. They stated that the BAFF-R was expressed at a high level on all B-cells and at very low levels on T-cells in human peripheral blood. It is also expressed in tonsil B-cells, but B-cells with a GC phenotype ($CD38^+$, $CD27^+$, $CD39^-$, $CD24^-$ and IgM^-) exhibited lower levels of BAFF-R according to flow cytometry [21]. Intense staining of B-cell follicles and weaker staining of the GCs were observed in the immunohistochemistry using frozen sections [21]. We demonstrated that BAFF-R was strongly expressed on B-cells situated both in the mantle zone and the marginal zones of the secondary lymphoid follicles and weakly expressed on GC B-cells occasionally

Table 1 Reactivity of 8A7 in 109 neoplastic lymphoid tissues according to immunohistochemistry (Positive cases/examined cases). *NLP-HL* nodular lymphocyte predominance Hodgkin lymphoma; *MC-CHL* mixed cellularity classical Hodgkin lymphoma; *NS-CHL* nodular sclerosis classical Hodgkin lymphoma

B-lymphoblastic lymphoma	0/3
Chronic lymphocytic leukemia/Small lymphocytic lymphoma	4/4
Mantle cell lymphoma	9/11
Follicular lymphoma	10/14
Grade 1	4/4
Grade 2	4/4
Grade 3	2/6
Diffuse large B-cell lymphoma	11/25
Marginal zone B-cell lymphoma	8/10
Lymphoplasmacytic lymphoma	2/2
Plasma cell myeloma	0/2
Burkitt lymphoma	0/9
T-lymphoblastic lymphoma	0/3
Angioimmunoblastic T-cell lymphoma	0/4
Peripheral T-cell lymphoma, unspecified	0/5
Adult T-cell lymphoma	0/2
Anaplastic large cell lymphoma	0/1
NK/T cell lymphoma	0/4
Hodgkin lymphoma	0/10
NLP-HL	0/3
MC-CHL	0/4
NS-CHL	0/3

in the GCs. The intensity of BAFF-R in GC B-cells may vary between each GC. Marginal zone B-cells have somatically hypermutated immunoglobulin (Ig) genes and express CD27 at a level equivalent to memory B-cells [10]. It is widely considered that marginal zone B-cell development and survival are likely to directly or indirectly depend on BAFF [13]. Since the present data indicate that marginal B-cells express BAFF-R, it is likely that BAFF directly contributes to the maturation of marginal zone B-cells. BAFF-R was also expressed strongly on mantle zone B-cells, which are naive B-cells that exhibit unmutated Ig genes and mainly co-express IgM and IgD [11]. On the other hand, GC B-cells that undergo affinity maturation of their antigen receptors and express CD10 and CD38 [25] were observed to be negative or weakly positive for BAFF-R. Thus, BAFF-R is widely distributed on un-stimulated B-cells and antigen-stimulated B-cells during B cell differentiation, except for GC B-cells. This pattern of BAFF-R expression during different stages of B-cell differentiation seemed to be similar to that of Bcl-2 expression. GC B-cells express low levels of BAFF-R and the anti-apoptotic factor Bcl-2, and high levels of the apoptotic factor Fas [17, 39].

Novak et al. reported the cell surface expression of BAFF-R on both CD5 (+) peripheral blood B-cells as well as CD5 (−) peripheral blood B-cells [23]. Mice transgenic for TACI-Ig, and BAFF-deficient mice display a developmental block of B-cell maturation in the periphery, leading to a severe depletion of marginal zone and follicular B2 B-cells, but not of peritoneal CD5 (+) B1 B-cells [4, 13, 29]. Interactions between BAFF and BAFF-R may be needed for CD5 (+) B1 B-cell maturation as much as CD5 (−) B2 B-cell maturation in humans.

The reactivity of anti-BAFF-R mAb against neoplastic lymphoid tissue is of considerable interest. It is likely that BAFF-R expression was only found in B-cell lymphoma, but not in T/NK-cell lymphomas, for reasons related to the fact that BAFF-R expression is normally found only on healthy B-cells [21]. Only a small number of studies reporting BAFF-R expression in malignant B-cells have appeared to date. Seven of seven B-CLL samples, as well as normal B-cells, expressed BAFF-R mRNA [22]. None of the five MM cell-lines but two of the three mononuclear cells of patients with MM expressed cell surface BAFF-R [23]. Six of six NHLs, including CLL/SLL, MCL, FL, BL, and DLBCL, expressed BAFF-R mRNA [7]. In the present study, however, we demonstrated somewhat different results for BAFF-R expression.

Most of the low-grade B-cell neoplasms of B-CLL/SLL, MCL, LPL and MZBCL strongly exhibited BAFF-R. Among them, MCL and MZBCL are believed to be neoplasms derived from mantle zone B-cells and marginal zone B-cells, respectively. The normal counterpart cells of B-CLL/SLL are a neoplasm of CD5 (+) B-cells of the peripheral blood [15, 29]. These normal counterpart cells are all BAFF-R (+) and these B-cell neoplasms seemed to maintain BAFF-R expression. Low-grade B-cell lymphomas may require the interaction of BAFF and BAFF-R for survival and proliferation of the neoplastic B-cells.

Although normal GC B-cells exhibited a negative reaction or an occasionally weakly positive reaction for 8A7, both grade 1 and 2 FLs strongly expressed BAFF-R. FL consists of small-cleaved lymphoma cells with intermingled large sized centroblasts. Grade 1 and 2 FLs include less than 50 centroblasts and 50–150 centroblasts per ten high-power fields, respectively. Both grades 1 and 2 FLs retain a follicular growth pattern supported by a network of follicular dendritic cells (FDCs), and the lymphoma cells express CD20, CD10, Bcl-2 and Bcl-6 [20]. It has recently been shown that FDCs express BAFF [6]. On the other hand, in grade 3 FL, 2/3 in grade 3a and 0/3 in grade 3b were positive for 8A7. This may indicate that lymphoma cells of grade 1 and 2 FLs require the interaction of BAFF and BAFF-R for their survival and growth. Certain lymphoma cells of some grade 3 FL act autonomically in terms of proliferation.

BAFF-R was expressed in a lower number of cases of aggressive B-cell lymphomas. LBL and BL were negative for 8A7. Eleven out of 25 DLBCLs exhibited a positive reaction with anti-BAFF-R mAb, which supports the recent report by He et al. [7]. Among these, the expression of BAFF-R was found in CD5 (+) DLBCL as well as CD5 (+) CLL/SLL and MCL. BAFF-R (+) in many cases of CD5 (+) B-cell neoplasms was independent of their aggressiveness and clinical behavior. These findings may prove to be useful for the continual improvement of understanding of the biology of CD5 (+) B-cells and B-cell neoplasms, especially for CD5 (+) DLBCL, which is reported to have a poorer clinical outcome than CD5 (−) DLBCL [19, 36].

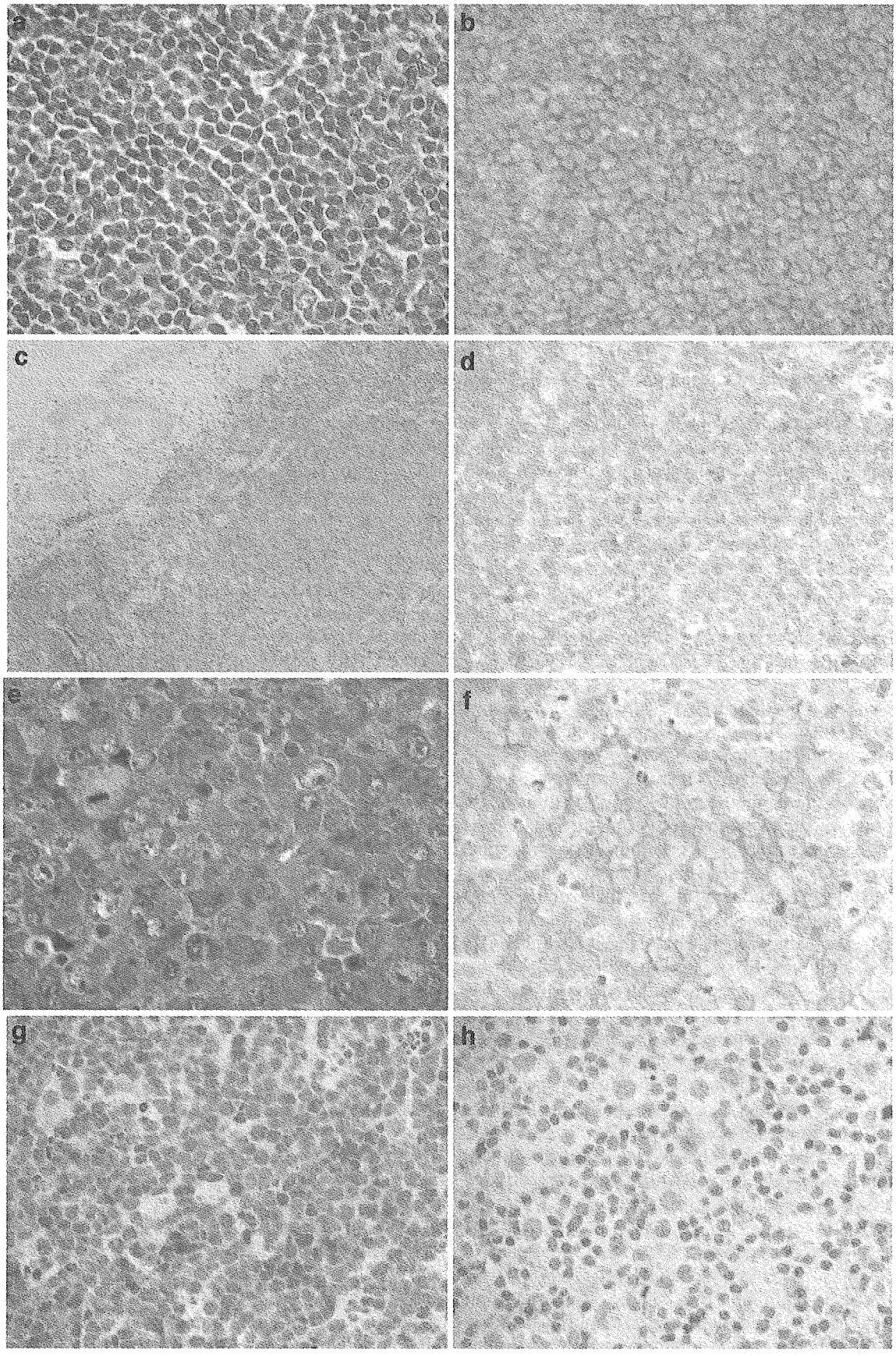
a
b
c
d
e
f
g
h

◀ **Fig. 3** BAFF-R expression in neoplastic lymphoid tissues according to immunohistochemistry (IHC) on the paraffin-embedded sections (strept/ABC method). 8A7 is strongly expressed in CD20 (+) CD5 (+) cyclin D1 (+) mantle cell lymphoma (**a**: HE, **b**: IHC, original magnification ×200). 8A7 reacts with the lymphoma cells of gastric MALT lymphoma, but not with the glandular epithelium (**c**: IHC, ×50; **d**: IHC, ×200). 8A7 expressed on some of the lymphoma cells of CD20 (+) CD5 (+) diffuse large B-cell lymphoma (**e**: HE, **f**: IHC, ×200) (**g**: IHC, ×200). Expression of 8A7 is not found in Hodgkin/Reed-Sternberg cells of Hodgkin lymphoma, but in a small number of small lymphocytes (**h**: IHC, ×200) Burkitt lymphoma is negative for 8A7

We analyzed the clinical profiling between BAFF-R (+) and BAFF-R (−) subgroups in all DLBCL examined. When analyzing these between the BAFF-R (+) and BA FF-R (−) subgroups in CD5 (−) CD10 (−) DLBCL, we found a significant difference in LDH. The number of patients with LDH >2-fold of the normal limit in the BAFF-R (+) subgroups was greater than that in the BAFF-R (−) subgroup (detailed data not shown). This may mean that the volume of lymphoma cells in patients with BAFF-R (+) DLBCL is high and may affect the treatment strategy for patients with BAFF-R (+) DLBCL. We found no significant differences in the overall survival curves between the two subgroups due to the small number of patients in this study, and more cases are needed for an accurate estimation. BAFF-R is a possible marker for sub-grouping of DLBCL. On the other hand, two out of three CD5 (+) DLBCL exhibited more than 2-fold the normal limit of LDH, but both cases of CD10 (+) DLBCL exhibited LDH within the normal limit.

The HRS cells of all cases of HL including NLP-HL, MC-CHL and NS-CHL were negative for BAFF-R. This is a marked difference from the finding that more than half of HL cases express the bcl-2 protein, an anti-apoptotic factor [26]. HL is a neoplasm derived from GC B-cells with a hypermutated Ig gene, as disclosed by single cell PCR analysis, and lacks Ig mRNA, which is different from the cases of DLBCL [16, 38]. Since the expression of BAFF-R is regulated by immunoglobulin, it is possible that HL is not able to express BAFF-R [31]. It is, however, odd that the NLP-HL that expresses Ig was also negative for 8A7.

In conclusion, we developed an anti-human BAFF-R mAb and addressed its reactivity and distribution in normal and malignant lymphoid tissues by performing immunohistochemistry with paraffin-embedded tissues. BAFF-R was found to be expressed on B-cells situated in the mantle and marginal zones, but not on B-cells in GC. We demonstrated that BAFF-R was expressed on most low-grade B-cell neoplasms and in some DLBCL.

Acknowledgements We thank Dr. Hajime Karasuyama for the pBCMGSneo expression vector, Dr. Hidefumi Kojima for helpful discussion, and Ms. Yumiko Kanno for participating in technical assistance. We also thank the Laboratory Animal Research Center and the Laboratory of Analytical Instruments, Institute for Medical Science, Dokkyo University School of Medicine, for the use of their facilities.

A grant-in-aid for Scientic Research (c) from the Ministry of Education, Culture, Sports, Science and Technology of Japan (KA KENHI 16590410 to T.K.) and The Science Research Promotion Fund from the Promotion and Mutual Aid Corporation for Private Schools of Japan (to T.K.)

References

1. Avery DT, Kalled SL, Ellyard JI et al (2003) BAFF selectively enhances the survival of plasmablasts generated from human memory B cells. J Clin invest 112:286–297
2. Briones J, Timmerman JM, Hilbert DM, Levy R (2002) BLyS and BlyS receptor expression in non-Hodgkin's lymphoma. Exp Hematol 30:135–141
3. Gross JA, Johnston J, Mudri S, Enselman R, Dillon SR, Madden K, Xu W, Parrish-Novak J, Foster D, Lofton-Day C, Moore M, Littau A, Grossman A, Haugen H, Foley K, Blumberg H, Harrison K, Kindsvogel W, Clegg CH (2000) TACI and BCMA are receptors for a TNF homologue implicated in B-cell autoimmune disease. Nature 404:995–999
4. Gross JA, Dillon SR, Mudri S, Johnston J, Littau A, Roque R, Rixon M, Schou O, Foley KP, Haugen H, McMillen S, Waggie K, Schreckhise RW, Shoemaker K, Vu T, Moore M, Grossman A, Clegg CH (2001) TACI-Ig neutralizes molecules critical for B cell development and autoimmune disease. Impaired B cell maturation in mice lacking BLyS. Immunity 15:289–302
5. Hase H, Kanno Y, Kojima H, Morimoto C, Okumura K, Kobata T (2002) CD27 and CD40 inhibit p53-independent mitochondrial pathways in apoptosis of B cells induced by B cell receptor ligation. J Biol Chem 277:46950–46958
6. Hase H, Kanno Y, Kojima M, Hasegawa K, Sakurai D, Kojima H, Tsuchiya N, Tokunaga K, Masawa N, Azuma M, Okumura K, Kobata T (2004) BAFF/BLyS can potentiate B-cell selection with the B-cell co-receptor complex. Blood 103:2257–2265
7. He B, Chadburn A, Jou E, Schattner EJ, Knowles DM, Cerutti A (2004) Lymphoma B cells evade apoptosis through the TNF family members BAFF/BLyS and APRIL. J Immunol 172:3268–3279
8. Karasuyama H, Kudo A, Melcher F (1990) The proteins encoded by the VpreB and lambda 5 pre-B cell-specific genes can associate with each other and with mu heavy chain. J Exp Med 172:969–972
9. Khare SD, Sarosi I, Xia XZ, McCabe S, Miner K, Solovyev I, Hawkins N, Kelley M, Chang D, Van G, Ross L, Delaney J, Wang L, Lacey D, Boyle WJ, Hsu H (2000) Severe B cell hyperplasia and autoimmune disease in TALL-1 transgenic mice. Proc Natl Acad Sci USA 97:3370–3375
10. Klein U, Rajewsky K, Kuppers R (1998) Human immunoglobulin (Ig)M+IgD+ peripheral blood B cells expressing the CD27 cell surface antigen carry somatically mutated variable region genes: CD27 as a general marker for somatically mutated (memory) B cells. J Exp Med 188:1679–1689
11. Klein U, Goossens T, Fischer M, Kanzler H, Braeuninger A, Rajewsky K, Kuppers R (1998) Somatic hypermutation in normal and transformed human B cells. Immunol Rev 162:261–280
12. Mackay F, Woodcock SA, Lawton P et al. (1999) Mice transgenic for BAFF develop lymphocytic disorders along with autoimmune manifestations. J Exp Med 190:1697–1710
13. Mackay F, Schneider P, Rennert P, Browning JL (2003) BAFF and APRIL: a tutorial on B cell survival. Annu Rev Immunol 21:231–264
14. Madry C, Laabi Y, Callebaut I et al. (1988) The characterization of murine BCMA gene defines it as a new member of the tumor necrosis factor superfamily. Int Immunol 10:1063–1702
15. Maes B, De Wolf-Peeters C (2002) Marginal zone cell lymphoma—an update on recent advances. Histopathology 40:117–126
16. Marafioti T, Hummel M, Foss HD, Laumen H, Korbjuhn P, Anagnostopoulos I, Lammert H, Demel G, Theil J, Wirth T, Stein H (2000) Hodgkin and Reed-Sternberg cells represent an expansion of a single clone originating from a germinal center B-cell with functional immunoglobulin gene rearrangements but defective immunoglobulin transcription. Blood 95:1443–1450

17. Martinez-Valdez H, Guret C, de Bouteiller O, Fugier I, Banchereau J, Liu YJ (1996) Human germinal center B cells express the apoptosis-inducing genes Fas, c-myc, P53, and Bax but not the survival gene bcl-2. J Exp Med 183:971–977
18. Moore PA, Belvedere O, Orr A, Pieri K, LaFleur DW, Feng P, Soppet D, Charters M, Gentz R, Parmelee D, Li Y, Galperina O, Giri J, Roschke V, Nardelli B, Carrell J, Sosnovtseva S, Greenfield W, Ruben SM, Olsen HS, Fikes J, Hilbert DM (1999) BLyS: member of the tumor necrosis factor family and B lymphocyte stimulator. Science 285:260–263
19. Nakamura N, Abe M (2003) Histogenesis of CD5-positive and CD5-negative B-cell neoplasms on the aspect of somatic mutation of immunoglobulin heavy chain gene variable region. Fukushima J Med Sci 49:55–67
20. Nathwani BN, Harris NL, Weisenburger D, Isaacson PG, Piris MA, Berger F, Muller-Hermalink HK, Swerdlow SH (2001) Follicular lymphoma. In: Jaffe ES, Harris NL, Stein H, Vardiman JW (eds) Tumours of haematopoietic and lymphoid tissues. IARC Press, Lyon, France pp 162–167
21. Ng LG, Sutherland AP, Newton R, Qian F, Cachero TG, Scott ML, Thompson JS, Wheway J, Chtanova T, Groom J, Sutton IJ, Xin C, Tangye SG, Kalled SL, Mackay F, Mackay CR (2004) B cell-activating factor belonging to the TNF family (BAFF)-R is the principal BAFF receptor facilitating BAFF costimulation of circulating T and B cells. J Immunol 173:807–817
22. Novak AJ, Bram RJ, Kay NE, Jelinek DF (2002) Aberrant expression of B-lymphocyte stimulator by B chronic lymphocytic leukemia cells: a mechanism for survival. Blood 100: 2973–2979
23. Novak AJ, Darce JR, Arendt BK, Harder B, Henderson K, Kindsvogel W, Gross JA, Greipp PR, Jelinek DF (2004) Expression of BCMA, TACI, and BAFF-R in multiple myeloma: a mechanism for growth and survival. Blood 103:689–694
24. O'Connor BP, Raman VS, Erickson LD, Cook WJ, Weaver LK, Ahonen C, Lin L-L, Mantchev GT, Bram RJ, Noelle RJ (2004) BCMA is essential for the survival of long-lived bone marrow plasma cells. J Exp Med 199:91–97
25. Pascual V, Liu YJ, Magalski A, de Bouteiller O, Banchereau J, Capra JD (1994) Analysis of somatic mutation in five B cell subsets of human tonsil. J Exp Med 180:329–339
26. Rassidakis GZ, Medeiros LJ, Vassilakopoulos TP, Viviani S, Bonfante V, Nadali G, Herling M, Angelopoulou MK, Giardini R, Chilosi M, Kittas C, McDonnell TJ, Bonadonna G, Gianni AM, Pizzolo G, Pangalis GA, Cabanillas F, Sarris AH (2002) BCL-2 expression in Hodgkin and Reed-Sternberg cells of classical Hodgkin disease predicts a poorer prognosis in patients treated with ABVD or equivalent regimens. Blood 100:3935–3941
27. Schiemann B, Gommerman JL, Vora K, Cachero TG, Shulga-Morskaya S, Dobles M, Frew E, Scott ML (2001) An essential role for BAFF in the normal development of B cells through a BCMA-independent pathway. Science 293:2111–2114
28. Schneider P, MacKay F, Steiner V, Hofmann K, Bodmer JL, Holler N, Ambrose C, Lawton P, Bixler S, Acha-Orbea H, Valmori D, Romero P, Werner-Favre C, Zubler RH, Browning JL, Tschopp J (1999) BAFF, a novel ligand of the tumor necrosis factor family, stimulates B cell growth. J Exp Med 189:1747–1756
29. Schneider P, Takatsuka H, Wilson A, Mackay F, Tardivel A, Lens S, Cachero TG, Finke D, Beermann F, Tschopp J (2001) Maturation of marginal zone and follicular B cells requires B cell activating factor of the tumor necrosis factor family and is independent of B cell maturation antigen. J Exp Med 194:1691–1697
30. Seshasayee D, Valdez P, Yan M, Dixit VM, Tumas D, Grewal IS (2003) Loss of TACI causes fatal lymphoproliferation and autoimmunity, establishing TACI as as inhibitory BLys receptor. Immunity 18:279–288
31. Smith SH, Cancro MP (2003) Cutting edge: B cell receptor signals regulate BLyS receptor levels in mature B cells and their immediate progenitors. J Immunol 170:5820–5823
32. Thompson JS, Bixler SA, Qian F et al. (2001) BAFF-R, a newly identified TNF receptor that specifically interacts with BAFF. Science 293:2108–2111
33. von Bulow GU, Bram RJ (1997) NF-AT activation induced by a CAML-interacting member of the tumor necrosis factor superfamily. Science 278:138–141
34. von Bulow GU, van Deursen JM, Bram RJ (2001) Regulation of the T-independent humoral response by TACI. Immunity 14: 573–582
35. Vora KA, Wang LC, Rao SP, Liu ZY, Majeau GR, Cutler AH, Hochman PS, Scott ML, Kalled SL (2003) Germinal centers formed in the absence of B cell-activating factor belonging to the TNF family exhibit impaired maturation and function. J Immunol 171:547–551
36. Yamaguchi M, Seto M, Okamoto M, Ichinohasama R, Nakamura N, Yoshino T, Suzumiya J, Murase T, Miura I, Akasaka T, Tamaru J, Suzuki R, Kagami Y, Hirano M, Morishima Y, Ueda R, Shiku H, Nakamura S (2002) De novo CD5+ diffuse large B-cell lymphoma: a clinicopathologic study of 109 patients. Blood 99:815–821
37. Yan M, Wang H, Chan B et al. (2001) Activation and accumulation of B-cells in TACI-deficient mice. Nat Immunol 2:638–645
38. Yatabe Y, Oka K, Asai J, Mori N (1996) Poor correlation between clonal immunoglobulin gene rearrangement and immunoglobulin gene transcription in Hodgkin's disease. Am J Pathol 149:1351–1361
39. Yoshino T, Kondo E, Cao L, Takahashi K, Hayashi K, Nomura S, Akagi T (1994) Inverse expression of bcl-2 protein and Fas antigen in lymphoblasts in peripheral lymph nodes and activated peripheral blood T and B lymphocytes. Blood 83:1856–1861

A novel small molecular weight compound with a carbazole structure that demonstrates potent human immunodeficiency virus type-1 integrase inhibitory activity

Hua Yan[1], Tomoko Chiba Mizutani[1], Nobuhiko Nomura[2], Tadakazu Takakura[2], Yoshihiro Kitamura[3], Hideka Miura[1], Masako Nishizawa[1], Masashi Tatsumi[1], Naoki Yamamoto[1] and Wataru Sugiura[1*]

[1]AIDS Research Center, National Institute of Infectious Diseases, Tokyo, Japan
[2]Research and Discovery Laboratories, Toyama Chemical Co. Ltd., Toyama, Japan
[3]Division of Infectious Diseases, Advanced Clinical Research Center, Institute of Medical Science, University of Tokyo, Japan.

*Corresponding author: Tel: +81 42 561 0771; Fax: +81 42 561 7746; E-mail: wsugiura@nih.go.jp

The integration of reverse transcribed proviral DNA into a host genome is an essential event in the human immunodeficiency virus type 1 (HIV-1) replication life cycle. Therefore, the viral enzyme integrase (IN), which plays a crucial role in the integration event, has been an attractive target of anti-retroviral drugs. Several IN inhibitory compounds have been reported previously, yet none has been successful in clinical use. To find a new, more successful IN inhibitor, we screened a diverse library of 12 000 small molecular weight compounds randomly by *in vitro* strand-transfer assay. We identified a series of substituted carbazoles that exhibit strand-transfer inhibitory activity at low micromolar concentrations. Of these, the most potent compound exhibited an IC_{50} of 5.00 ±3.31 μM (CA-0). To analyse the structural determinants of strand-transfer inhibitory activity of the carbazole derivatives, we selected 23 such derivatives from our compound library and performed further analyses. Of these 23 compounds, six showed strong strand-transfer inhibition. The inhibition kinetics analyses and ethidium bromide displacement assays indicated that the carbazole derivatives are competitive inhibitors and not intercalators. An HeLa4.5/LTR-nEGFP cell line was employed to evaluate *in vitro* virus replication inhibition of the carbazole derivatives, and IC_{50} levels ranged from 0.48–1.52 μM. Thus, it is possible that carbazole derivatives, which possess structures different from previously-reported IN inhibitors, may become novel lead compounds in the development of IN inhibitors.

Keywords: integrase inhibitor, carbazole, HIV-1, antiretroviral drug

Introduction

Human immunodeficiency virus type 1 (HIV-1), causative agent of acquired immunodeficiency syndrome (AIDS), possesses three critical enzymes for replication. These are protease (PR), reverse transcriptase (RT), and integrase (IN) (Ruscetti, 1985; Kohl *et al.*, 1988; LaFemina *et al.*, 1992). As inactivating any of these enzymes may negate the infectivity of HIV-1, the enzymes have been targets of anti-retroviral drug development. Indeed, great progress in anti-retroviral drug discovery has been achieved in recent decades, and today 10 RT inhibitors and eight PR inhibitors (De Clercq, 1992; Tronchet & Seman, 2003; Balzarini, 2004; Imamichi, 2004) are available for anti-retroviral treatments. The third enzyme, IN, has also been a major target of inhibitor development. L-708,906 and L-731,988, which possess diketo acid moieties within their structures, were the first IN-specific inhibitors discovered (Pommier *et al.*, 2000; Dayam & Neamati, 2003; Pluymers *et al.*, 2002; Hazuda *et al.*, 2000). S-1360 and L-870,810, which also have diketo acid moieties, are IN inhibitors that have reached clinical Phase I/II trials for the first time (Johnson *et al.*, 2004; Hazuda *et al.*, 2004). However, although there have been large advances in the development of IN inhibitors, further research and analysis is required to develop clinically usable compounds.

Integrase (IN), the leading target of novel anti-retroviral inhibitor development, is the enzyme responsible for integration, wherein reverse transcribed HIV-DNA is inserted into a host genome, and is critical for viral replication, which in turn establishes latency and chronic infection (Chun *et al.*, 1995). IN is composed of three distinct

domains – the N-terminal domain (amino acids 1–50) with a zinc-binding motif (Schauer & Billich, 1992; Burke *et al.*, 1992), the catalytic core domain (amino acids 50–212) with polynucleotidyl transfer activity and sequence-specific endonuclease activity (Engelman & Craigie, 1992; Engelman *et al.*, 1994) and the C-terminal domain (amino acids 212–288), which has been thought to relate to nonspecific DNA binding (Khan *et al.*, 1991; Woerner & Marcus-Sekura, 1993).

At present, the function and structure of each domain has not been fully understood. The most well-analysed domain is the catalytic core domain, and its active site has highly conserved amino acidic residues Asp64, Asp116 and Glu152, which are critical for polynucleotidyl transfer activity (LaFemina *et al.*, 1992; Engelman *et al.*, 1995). Previously reported potent IN inhibitors L-708,906, L-731,988, L-801,810, S-1360 and 5-CITEP are all targeted to this domain. These inhibitors bind to the active site, displace divalent metal ion Mg^{2+} from the active site and inactivate the catalytic activity of IN (Grobler *et al.*, 2002; Dayam & Neamati, 2003; Goldgur *et al.*, 1999; Johnson *et al.*, 2004). No specific inhibitors have been reported for the N-terminal and C-terminal domains.

In the present study we attempted to identify novel IN inhibitory compounds, and therefore we conducted a random screening of a library of small molecular weight compounds. As a result, we discovered a series of novel IN inhibitory compounds with carbazole structures, that are quite different from previously reported inhibitory compounds.

Materials and methods

Preparation of integrase

The sequence coding the NL4-3 integrase (IN) was cloned into pET28b(+) (Novagen, Madison, WI, USA), generating pET-IN that codes NL4-3 IN with a hexa-histidine tag at the N-terminus. *Escherichia coli* strain Rosetta (DE3) (Novagen) transformed with pET-IN was grown in 1 l of Super Broth (Biofluids, Camarillo, CA, USA) containing 100 μg/ml kanamycin at 30°C until the optical density of the culture had reached between 0.5 and 0.7 at 600 nm. The recombinant protein expression was induced by isopropyl-1-thio-D-galactopyranoside. After incubation for 3 h, the cells were harvested and resuspended in 100 ml of preparation buffer (20 mM Tris-HCl, pH 8.0, 0.5 M NaCl) and disrupted by sonication. Following high-speed centrifugation at 40 000×g for 45 min at 4°C, the pellet was homogenized in GBB buffer (50 mM Tris-HCl, pH 8.0, 6 M Guanidine HCl and 2 mM 2-ME). The residual pellet was again sonicated and centrifuged at 40 000×g for 30 min at 4°C.

The supernatant was filtered through a 0.22 μm filter and mixed with 1 ml of nickel-affinity resin (Sigma, St. Louis, MO, USA), and incubated overnight at 4°C. The resin was washed twice by mixing with 20 ml of GBB containing 5 mM imidazole (Sigma). The protein was eluted with GBB containing 1 M imidazole. The fractions containing integrase were pooled and 0.5 M EDTA was added to a final concentration of 5 mM. This eluted protein was then sequentially dialysed against (i) 6 M guanidine HCl, 50 mM Tris-HCl (pH 8.0), 2 mM 2-ME, 1 mM EDTA for 2 h at room temperature, (ii) 6 M guanidine HCl, 50 mM Tris-HCl (pH 8.0), 10 mM DTT, 1 mM EDTA for 16 h at room temperature, (iii) 4 M urea, 50 mM Tris-HCl (pH 8.0), 0.5 M NaCl, 1 mM DTT, 0.1 mM EDTA for 16 h at 4°C, (iv) 2 M urea, 50 mM Tris-HCl (pH 8.0), 0.5 M NaCl, 1 mM DTT, 0.1 mM EDTA, 20% (w/v) glycerol for 16 h at 4°C, (v) 1 M urea, 50 mM Tris-HCl (pH 8.0), 1 M NaCl, 1 mM DTT, 0.1 mM EDTA, 15 mM 3-[(3-cholamidopropyl) dimethylammonio]-1-propanesulfonate (CHAPS), 20% (w/v) glycerol for 16 h at 4°C, and (vi) 50 mM Tris-HCl (pH 8.0), 1 M NaCl, 1 mM DTT, 0.1 mM EDTA, 15 mM CHAPS, 20% (w/v) glycerol for 16 h at 4°C. The final preparation was stored at −80°C.

The purified enzyme activity was confirmed and evaluated by strand-transfer assay using M8 apparatus (IGEN, Gaithersburg, MD, USA).

Preparation of test compounds

A diverse library of 12 000 small-molecule compounds was supplied by Toyama Chemicals Co. Ltd. (Toyama, Japan). All test compounds were dissolved in DMSO and adjusted to 2 mM concentration. S-1360 was synthesized as positive control for strand transfer assay.

Construction of strand-transfer assay

Two different strand-transfer assay systems were employed in the IN inhibitor screening trial. For the first screening step, an M8 apparatus and strand-transfer assay kit, ORIGEN HIV integrase assay (IGEN), was used. In brief, magnetic beads coated with 29 mer donor double-stranded DNA (dsDNA) were mixed with purified IN (15 pmol), followed by adding the test compound and 20 mer target dsDNA tagged with ruthenium, conducting electronically inducible fluorescence chemistry, and incubating for 1 h at 37°C. Subsequently, the entire reaction solution was applied to the M8 apparatus, and then strand-transfer products were captured by a magnet in the flow-circuit of the equipment. The amount of the strand-transfer product was measured by ruthenium fluorescence activity. For the second and later screening steps, in-house strand-transfer assay was employed. The in-house assay was designed in 96-well plate format to achieve high-throughput screening.

The following donor and target DNA oligonucleotides were designed and used:
Donor-1 (D1): 5′-ACTGCTAGAGATTTTCCA-CACTGACTAAAAG-3′
Donor-2 (D2): Biotin-5′-CTTTTAGTCAGTGTGGA-AAATCTCTAGCA-3′
Target-1 (T1): 5′-CTAGAGATTTTCCACACTGACT-AAAAG-3′-Digoxigenin (DIG),
Target-2 (T2): 5′-CTTTTAGTCAGTGTGGAAAA-TCTCTAG-3′-DIG

To form dsDNA, the D1–D2 pair and the T1–T2 pair were mixed in the presence of 0.1 M NaCl and denatured for 10 min at 95°C, followed by an annealing process, gradual cooling down to room temperature. One pmol biotinulated donor dsDNA (D1–D2), 15 pmol IN protein and 5 µl test compounds (100 µM in DMSO) were mixed together in assay buffer (25 mM 3-(N-morpholino)-propanesulfonic acid, pH 7.2, 25 mM NaCl, 10 mM $MgCl_2$, 10 mM DTT, 5% PEG, 10% DMSO), followed by the addition of 0.75 pmol target dsDNA (T1–T2), and adjusted to a final volume of 100 µl and incubated for 1 h at 37°C. After the incubation, the mixture was adjusted to a final volume of 200 µl with ELISA buffer (20 mM Tris [pH 8.0], 0.4 M NaCl, 10 mM EDTA, 0.1 mg/ml sonicated DNA). To harvest the strand-transfer product, the mixture was transferred into a 96-well micro titre plate coated with streptavidin (PIERCE, Rockford, IL, USA), followed by adding an alkaline phosphatase conjugated anti-DIG antibody (Roche Diagnostics, Mannheim, Germany) and a disodium 3-(4-methoxyspiro{1,2-dioxetane-3,2′-(5′-chloro)tricyclo[3.3.1.1^{3,7}]decan}-4-yl) phenyl phosphate (CSPD) substrate (Roche). The lumino-intensity was quantified with a Luminous CT-9000D luminometer (DIA-IATRON, Tokyo, Japan).

In addition to the above two different strand-transfer assays, a strand-transfer assay with radioisotope labelled target DNA and SDS-PAGE was employed in order to visually confirm the strand-transfer inhibition (Craigie *et al.*, 1995). By use of T4 polynucleotide kinase (TAKARA BIO, Osaka, Japan), the 5′ end of 20 mer target oligonucleotide-A (5′-TGTGGAAAATCTCTAGCAGT-3′) was labelled with [γ-^{32}P] ATP (370 MBq/µl, Amersham Bioscience, Tokyo, Japan). After the labelling reaction was terminated by adding EDTA, complementary oligonucleotide-B (5′-ACTGCTAGAGATTTTCCACA-3′) was added, and dsDNA was formed by heat denaturation and gradual cooling to room temperature. Unincorporated [γ-^{32}P]ATP was removed by G-25 Column (Amersham Bioscience, Piscataway, NJ). The reaction products were applied to 20% denatured polyacrylamide gel electrophoresis (300V/25A). The result of the electrophoresis was analysed by BAS-2500 (Fuji film, Tokyo, Japan).

Inhibition kinetics of IN

To analyse the strand-transfer inhibition mechanism of the test compounds, whether the action is competitive inhibition or non-competitive inhibition, Michaelis-Menten constant (K_m) and maximum velocity (V_{max}) were evaluated. Strand-transfer inhibition was evaluated on eight different time points (0, 1, 3, 5, 7.5, 10, 15, and 20 min) with four different compound concentrations (0, 1, 5, 10 µM) and target DNA concentrations (0.167, 0.25, 0.5, and 1 pmol). The initial reaction rate constants of IN were determined by linear regression using linear data points of product concentration–time plots. K_m and V_{max} were calculated from the Y-axis intercept in a plot of the slopes of Lineweaver-Burk analysis.

Intercalative activity evaluation

To clarify the possibility of intercalative activity of test compounds, ethidium bromide (EtBr) displacement assay was carried out following the protocol reported previously (Cain *et al.*, 1978). In brief, 1 µM calf thymus DNA (Invitrogen, Carlsbad, CA, USA) was mixed with EtBr (final concentration at 1.26 µM) and reaction buffer (2 mM HEPES, 10 µM EDTA, 9.4 mM NaCl, pH 7.0), and incubated for 10 min at room temperature. After the incubation, test compounds were added into the calf thymus DNA–EtBr mixture at different concentrations (final concentrations of 0.01–1000 µM). Fluorescence intensity of each mixture was determined by Fluoroskan Ascent FL (Helsinki, Finland. Excited at 544 nm, emitted at 590 nm). Actinomycin D (ICN Biomedical, Aurora, OH, USA), which is known as an intercalator, was employed as the positive control of the assay.

Molecular modelling studies

Molecular modelling studies were carried out using SYBYL software Version 6.9.1 (Tripos, St. Louis, MO, USA) running on an SGI Fuel workstation equipped with 600-MHz R14000 processor (SGI, Mountain View, CA, USA).

Evaluation of *in vitro* antiviral activity.

To evaluate HIV-1 replication inhibition by selected test compounds, *in vitro* antiviral assays were performed using a HeLa4.5/nEGFP reporter cell line. The HeLa4.5/nEGFP reporter cell line was established by transfection of CD4 and LTR driven EGFP reporter protein into the HeLa cell line. HeLa4.5/nEGFP reporter cells were maintained with D-MEM (Sigma) containing 5% FCS (Hyclone, Logan, UT, USA), 500 µg/ml G418, 1 µg/ml blasticidin and 2 µg/ml puromycin.

One day before conducting the assay, $1x10^4$ HeLa4.5/nEGFP cells were seeded into clear bottom black 96-well plates (NUNC, Rochester, NY, USA) with

200 μl/well medium and incubated at 37°C, 5% CO_2. The next day, 1250 $TCID_{50}$ HXB2 were added in each well, followed by addition of the test compounds in final concentrations of 5, 1, 0.2, 0.04, 0.008, 0.0016, 0.00032, and 0.000064 μM. Forty-eight hours after infection, the cells were fixed by 3.2% formaldehyde and the nuclei of cells were stained by 10 μg/ml Hoechst33342 (Molecular Probes, Engene, OR, USA). EGFP positive cell number ($EGFP^+$) and Hoechst33342 positive cell number ($hoechst33342^+$) were determined by Cellomics Array Scan, HSC Systems (Beckman Coulter, Tokyo, Japan).

Inhibitory activity of each compound was determined by the following formula:

% inhibition = 1 − {($EGFP^+$ cell number with drug/$hoechst33342^+$ cell number with drug) − ($EGFP^+$ cell number without infection/$hoechst33342^+$ cell number without infection)}/{($EGFP^+$ cell number without drug/$hoechst33342^+$ cell number without drug) − ($EGFP^+$ cell number without infection/$hoechst33342^+$ cell number without infection)}.

Results

A small molecule bearing a carbazole moiety demonstrated strand-transfer inhibitory activity

A diverse library of 12 000 small-molecule compounds was screened for strand-transfer inhibitory activity at 100 μM concentration by M8 apparatus. Seventy-two compounds that demonstrated more than 80% strand-transfer-inhibition were selected and applied to the second screening using in-house strand-transfer assay. In the second screening, to confirm dose-dependent inhibition of the test compounds, each compound was tested at four different concentrations. Of the 72 compounds, a compound bearing a carbazole moiety, 8-chloro-2-[2-(dimethylamino)ethyl]-9-hydroxy-5-methylpyrrolo[3,4-c]carbazole-1,3(2H,6H)-dione (coded as **CA-0**), was found to demonstrate potent strand-transfer inhibitory activity (Figure 1A). As shown in Figure 1B, **CA-0** demonstrated clear dose-dependent inhibition of the strand-transfer reaction with an IC_{50} of 5.00 ±3.31 μM. The dose-dependent inhibition was also confirmed by SDS-PAGE with [γ-^{32}P] labelled target DNA. As demonstrated in Figure 1C, strand-transferred product bands diminished along with increased concentration of the inhibitor. IC_{50} value determined from intensities of the bands was 1.24 ±0.09 μM, which was consistent with that evaluated via the plate assay.

Strand-transfer inhibition of 23 carbazole derivatives, and the relationship between their structures and inhibitory activity

To understand the relationship between structure and strand-transfer inhibition activity, we selected 23 carbazole

Figure 1. Structure and strand transfer inhibitory activity of 8-chloro-2-[2-(dimethylamino) ethyl]-9-hydroxy-5-methylpyrrolo[3,4-c]carbazole-1,3(2H,6H)-dione (**CA-0**)

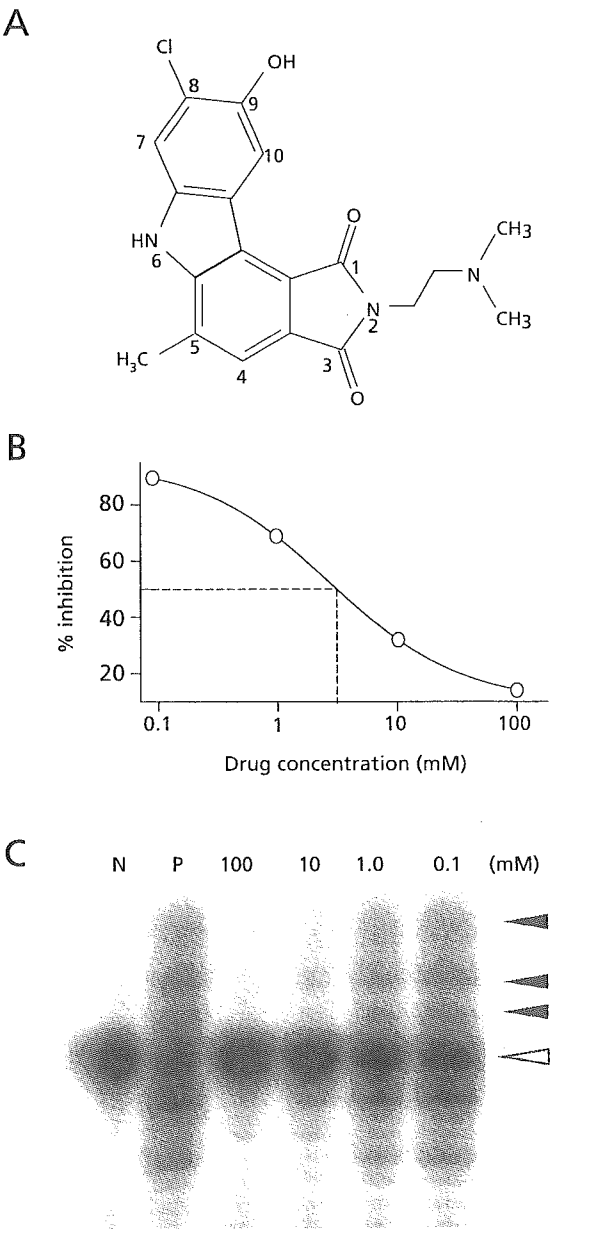

(A) The structure of **CA-0**, a strand transfer inhibitory compound identified from among a library of 12 000 small molecular weight compounds. It has a carbazole structure as a scaffold. The small numbers written beside the structure indicate the residue number of the compound. **(B)** A dose–response curve of **CA-0**. The dotted line indicates the IC_{50} point of the chemical, which was 5.00 ±3.31 μM. **(C)** A strand transfer assay by radioisotope-labelled oligonuceotide. Lane 1 "N" stands for the negative control, with only a radioisotope-labelled nucleotide. Lane 2 "P" stands for positive control, with radioisotope-labelled nucleotide and recombinant integrase. Lanes 3 to 6 were with inhibitor. The open triangle and solid triangle indicate labelled oligonucelotide and strand transfer products, respectively.

derivatives with different substituents. As demonstrated in Figure 2, all compounds had pyrrolo[3,4-c]carbazole structures as scaffolds, and all except **CA-5**, **CA-10** and **CA-19** had 2-dimethylaminoethyl group at position R2. Six of the 23 compounds demonstrated potent strand-transfer inhibition comparable to that of **CA-0**. These compounds were **CA-1**, **CA-4**, **CA-8**, **CA-9**, **CA-12** and **CA-13**. IC_{50} values of these test compounds were similar with positive control S-1360. Moderate inhibitory activities were observed in twelve compounds, **CA-2**, **CA-3**, **CA-7**, **CA-11**, **CA-14**, **CA-15**, **CA-16**, **CA-17**, **CA-18**, **CA-21**, **CA-22** and **CA-23**. Five compounds, **CA-5**, **CA-6**, **CA-10**, **CA-19** and **CA-20**, did not show significant inhibition, even at the highest concentration tested

Figure 2. Structures of **CA-0** and 23 carbazole derivatives evaluated for strand transfer inhibitory activity

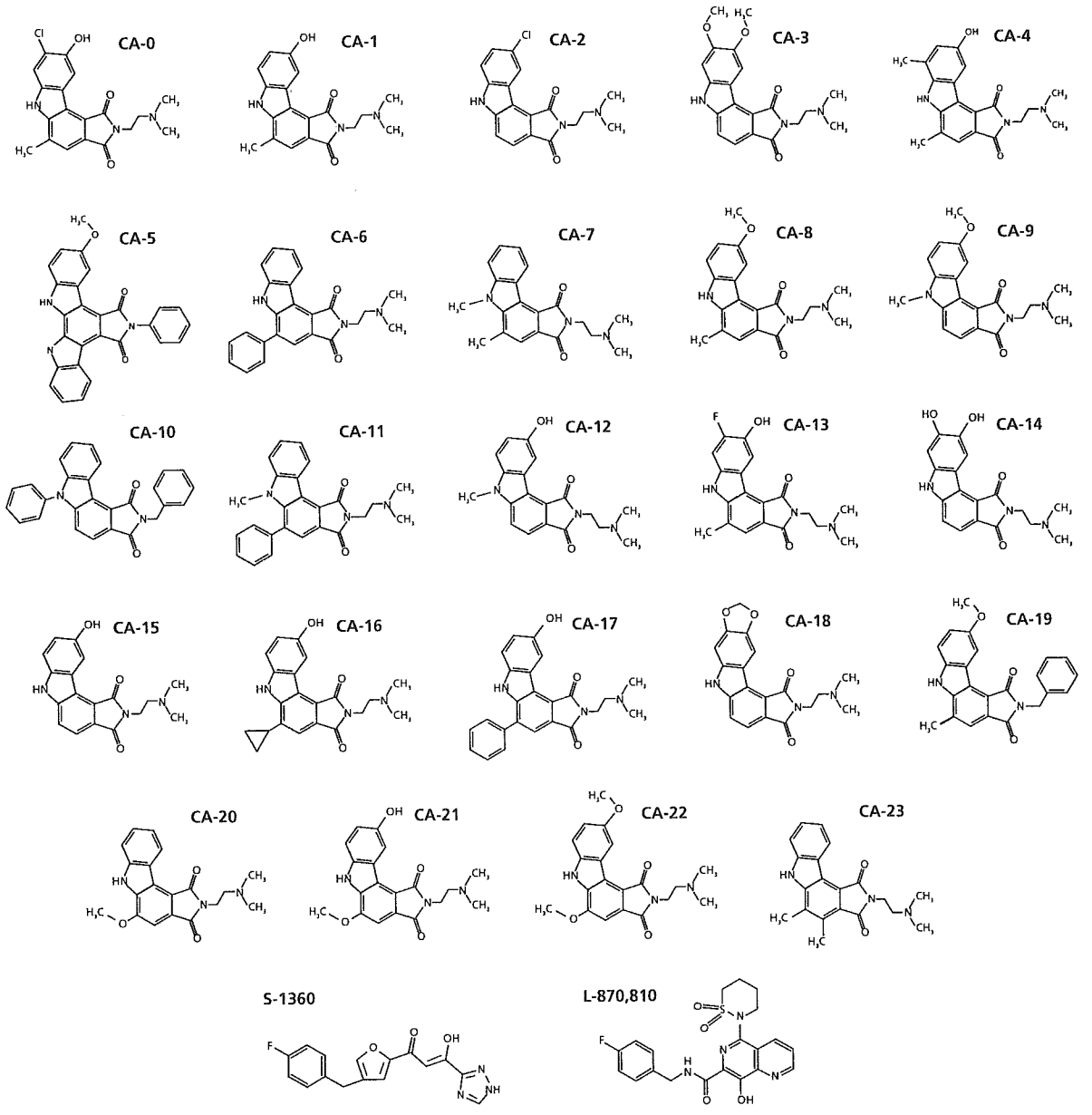

CA-0 and 23 related compounds with carbazole scaffold tested for strand-transfer inhibitory activities are depicted. S-1360 and L-870,810, which have previously been reported as potent IN inhibitors, are also shown.

(100 μM). The compounds that demonstrated potent strand-transfer inhibitory activity were also confirmed by gel-based assay, and IC_{50} values determined from the gel-based assay were consistent with the values determined via in-house plate assay (Table 1).

Carbazole derivatives are competitive inhibitors of integrase

To investigate the strand-transfer inhibitory mechanisms and kinetics of the compounds, we determined V_{max} and K_m of the inhibition by Lineweaver–Burke plot analyses. We selected two compounds, **CA-0** and **CA-13**, for the analyses. As summarized in Table 2, larger K_m values (nM) were observed with higher inhibitory concentration, whereas V_{max} values (RU/min) did not change and remained consistent at any inhibitory concentration (Figure 3). As shown in Figure 3A and 3B, data-fitted lines of different time points converged on the Y axis, indicating that **CA-0** and **CA-13** inhibited strand-transfer in a competitive manner.

Table 1. Strand transfer and *in vitro* viral replication inhibitory activities of carbazole derivatives

	IC_{50} in strand transfer assay		Anti-HIV activity
	Plate assay (μM)	Gel assay (μM)	IC_{50} (μM)
(A) High-inhibitory group			
CA-0	5.00 ±3.31	1.24 ±0.09	0.48 ±0.06
CA-13	4.38 ±2.78	1.13 ±0.21	0.51 ±0.12
CA-1	7.94 ±4.12	2.97 ±0.21	0.92 ±0.15
CA-4	8.99 ±3.39	6.34 ±0.89	1.52 ±0.46
CA-8	6.61 ±4.17	6.38 ±0.32	0.79 ±0.07
CA-9	4.42 ±1.87	4.10 ±0.46	0.80 ±0.11
CA-12	5.93 ±3.53	3.14 ±0.04	0.69 ±0.15
(B) Intermediate-inhibitory group			
CA-2	22.50 ±2.27	ND	ND
CA-3	72.69 ±5.44	ND	ND
CA-7	11.88 ±7.66	ND	ND
CA-11	57.00 ±3.13	ND	ND
CA-14	17.37 ±1.79	ND	ND
CA-15	27.28 ±9.10	ND	ND
CA-16	20.51 ±15.11	ND	ND
CA-17	50.64 ±19.02	ND	ND
CA-18	10.68 ±8.88	ND	ND
CA-21	25.01 ±10.60	ND	ND
CA-22	16.92 ±7.32	ND	ND
CA-23	16.94 ±7.82	ND	ND
(C) Intermediate-inhibitory group			
CA-5	>100	ND	ND
CA-6	>100	ND	ND
CA-10	>100	ND	ND
CA-19	>100	ND	ND
CA-20	>100	ND	ND
(D) Previously reported inhibitor			
S-1360	4.67 ±1.89	ND	ND

Underline, indicates original compound; IC_{50}, 50% inhibition concentration; ND, not done.

Carbazole derivates have not shown intercalative activity

Due to their planar structure and their manner of competitive inhibition, we were concerned that the compounds might have the intercalative activity to destroy substrate dsDNA, rather than binding to the IN to block its enzyme activity. To clear the possibility of the intercalation, EtBr displacement assay was carried out. Since EtBr intercalates into dsDNA and makes visualization possible by growing fluorescence under UV light, intercalative activity of the test compounds can be evaluated by whether the test compounds displace incorporated EtBr out from dsDNA. As shown in Figure 4, fluorescence intensity diminished in a dose-dependent manner by actinomycin D, a compound known as a potent intercalator. In contrast, our two test compounds **CA-0** and **CA-13** did not affect fluorescence intensity, even at the highest concentration of 1 mM, suggesting that **CA-0** and **CA-13** were not intercalators.

Antiviral activity

We employed a single replication infectivity assay using HeLa4.5/EGFP cells to investigate the potency of antiviral activity. IC_{50} values of **CA-0** and the six compounds were 0.48, 0.92, 1.52, 0.79, 0.8, 0.69, 0.51 μM, respectively. The IC_{50} values of all seven compounds were 5.5 to 10.4-fold lower than that of the strand transfer assay (Table 1A). The discrepancy in IC_{50} between the two assays can be explained by stoichiometry of the inhibitor and the target enzyme in the two assays, and the estimated amount of IN in-strand transfer assay was higher than in the

Table 2. Inhibition kinetics of representative carbazole compounds **CA-0** and **CA-13**

Chemical	Concentration	V_{max} (RU/min)	K_m (nM)
CA-0	10 μM	463.16 ±63.16	30.40 ±7.80
	5 μM	402.58 ±32.21	26.21 ±7.40
	1 μM	370.14 ±84.42	12.71 ±2.02
	0 μM	454.55 ±0.02	9.18 ±1.18
CA-13	10 μM	409.70 ±35.47	19.31 ±4.68
	5 μM	439.07 ±164.74	14.83 ±0.24
	1 μM	438.08 ±53.85	11.09 ±2.42
	0 μM	429.83 ±136.46	7.08 ±0.64

Figure 3. Inhibition kinetics assays of two representative carbazole derivatives, **CA-0** and **CA-13**

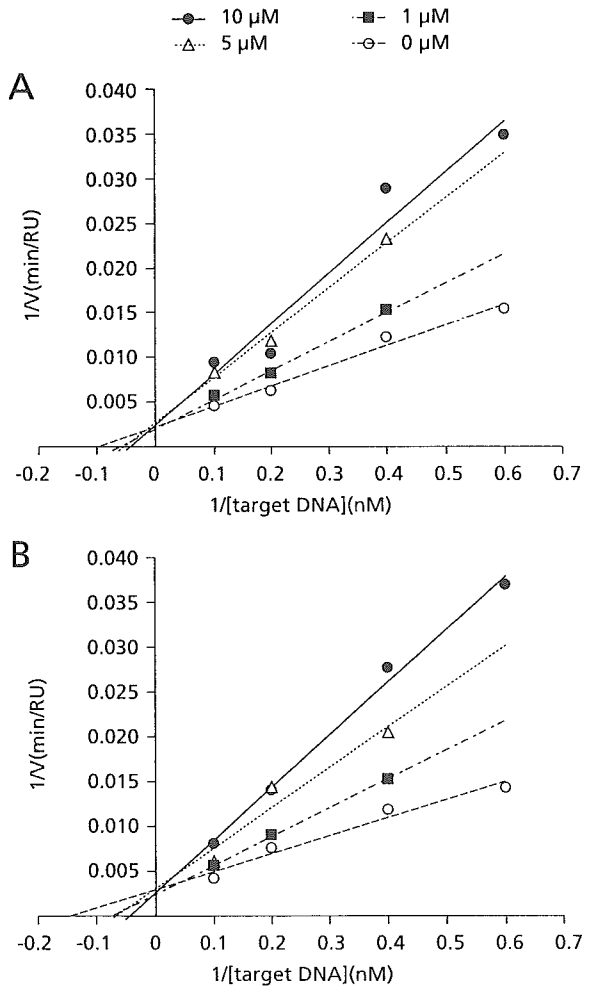

Lineweaver–Burke plot analyses of **(A) CA-0** and **(B) CA-13** are depicted.

Figure 4. Ethidium bromide displacement assays of two representative carbazole derivatives, **CA-0** and **CA-13**

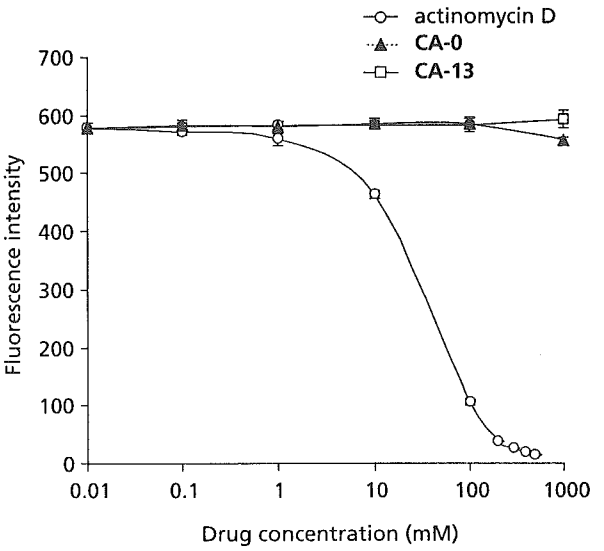

To evaluate intercalative activities of carbazole derivatives, ethidium bromide displacement assays were carried out for two representative compounds, **CA-0** and **CA-13**.

HeLa4.5/EGFP assay. Seven compounds exhibited considerable toxicity, suggesting that efforts toward decreasing toxicity are necessary for the further development of carbazole-based inhibitors.

Discussion

Carbazole, a fused phenyl-ring structure with hydrophobicity, has provided an interesting scaffold for the development of novel drugs. Staurosporine, discovered among microbial alkaloids, was the first carbazole derivative reported to demonstrate biological activity (Omura *et al.*, 1977; Furusaki *et al.*, 1978; Furusaki *et al.*, 1982), which was protein kinase C inhibition (Tamaoki *et al.*, 1986). Other carbazole derivatives have demonstrated various other activities, such as topoisomerase inhibition (Marotto *et al.*, 2002; Facompre *et al.*, 2002; Carrasco *et al.*, 2001), hypotensive activity (Furusaki *et al.*, 1982), platelet aggregation inhibition (Oka *et al.*, 1986), and anti-fungal activity (Sunthitikawinsakul *et al.*, 2003). In this report we present another possible activity of carbazole derivatives, that of HIV-1 integrase inhibitor.

As compounds with three or four fused aromatic ring structures have been reported to demonstrate intercalative activity (Fukui & Tanaka, 1996; Dziegielewski *et al.*, 2002), we initially suspected that our carbazole derivatives also have intercalative activities, penetrating and disturbing target dsDNA, resulting in pseudo strand-transfer inhibition. Indeed, several carbazole derivatives have been recognized to demonstrate intercalative activity (Facompre *et al.*, 2002; Long *et al.*, 2002). We confirmed that actinomycin D, which is a well-known intercalator (Ross *et al.*, 1979; Wilson & Jones, 1982), demonstrated strand-transfer inhibition in our assay (data not shown). However, taking into consideration the data that our carbazole derivatives inhibited strand-transfer in a competitive manner, and also that the compounds could not displace EtBr out from dsDNA, we assume that our derivatives bind to part of the IN molecule, to the region responsible for DNA target